



Functional liquid crystalline epoxy networks and composites: from materials design to applications

Yuzhan Li, Veronica Ambrogio, Pierfrancesco Cerruti, Monojoy Goswami, Zhou Yang, Michael R. Kessler & Orlando Rios

To cite this article: Yuzhan Li, Veronica Ambrogio, Pierfrancesco Cerruti, Monojoy Goswami, Zhou Yang, Michael R. Kessler & Orlando Rios (2021): Functional liquid crystalline epoxy networks and composites: from materials design to applications, International Materials Reviews, DOI: [10.1080/09506608.2021.1937811](https://doi.org/10.1080/09506608.2021.1937811)

To link to this article: <https://doi.org/10.1080/09506608.2021.1937811>



© 2021 The Author(s). Published by Informa UK Limited, trading as Taylor & Francis Group



Published online: 10 Jun 2021.



Submit your article to this journal [↗](#)



Article views: 485



View related articles [↗](#)



View Crossmark data [↗](#)

Functional liquid crystalline epoxy networks and composites: from materials design to applications

Yuzhan Li ^{a,b}, Veronica Ambrogio^c, Pierfrancesco Cerruti^d, Monojoy Goswami^e, Zhou Yang^a, Michael R. Kessler^f and Orlando Rios^g

^aSchool of Materials Science and Engineering, University of Science and Technology Beijing, Beijing, People's Republic of China; ^bBuildings and Transportation Science Division, Oak Ridge National Laboratory, Oak Ridge, TN, USA; ^cDepartment of Chemical, Materials and Production Engineering, University of Naples Federico II, Napoli, Italy; ^dInstitute for Polymers, Composites and Biomaterials, Italian National Research Council, Pozzuoli, Italy; ^eChemical Sciences Division, Oak Ridge National Laboratory, Oak Ridge, TN, USA; ^fDepartment of Mechanical Engineering, North Dakota State University, Fargo, ND, USA; ^gDepartment of Materials Science and Engineering, The University of Tennessee, Knoxville, TN, USA

ABSTRACT

Liquid crystalline epoxy networks (LCENs) are a class of materials that combine the useful benefits of both liquid crystals and epoxy networks exhibiting fascinating thermal, mechanical, and stimuli-responsive properties. They have emerged as a new platform for developing functional materials suitable for various applications, such as sensors, actuators, smart coatings and adhesives, tunable optical systems, and soft robotics. This article provides an overview of LCENs and their composites as functional materials, including their synthesis and characterisation, focusing on structure-processing–property relationships. We provide objective analyses on how materials engineers can use these relationships to develop LCENs with desired functionalities for targeted applications. Emerging areas, including advanced manufacturing and multi-functional design of LCENs are covered to show the overall progress in this field. We also survey the forward-looking status of LCEN research in designing novel materials for future technologies.

ARTICLE HISTORY

Received 16 January 2021
Accepted 26 May 2021

KEYWORDS

Epoxy resins; liquid crystals; liquid crystalline epoxy networks; composites; functional materials; orientation; stimuli-responsive; soft robotics

Introduction





Epoxy resins

Epoxy resins are an important class of polymers formed through the crosslinking of monomers containing epoxy groups, also known as oxirane or glycidyl groups [1]. The three-membered ring structure possesses considerable strain that provides the driving force for the epoxy to react rapidly with various curing agents, such as amines, anhydrides, carboxylic acids, alcohols, and thiols [2]. The curing reaction transforms the low molecular weight precursors into a three-dimensional network with infinite molecular weight. It results in materials with excellent thermal and mechanical properties, good chemical and moisture resistance, and outstanding adhesive performance. In addition, the ring-opening reaction of epoxy does not produce any volatile organic compound and allows for the formation of a network structure with low shrinkage [3]. These unique features, along with the wide selection of monomers and curing agents, make epoxy resins one of the most versatile polymers suitable for a broad range of applications, including coatings, adhesives, printed circuit board laminates, semiconductor encapsulates, and advanced composites [4].

The research and development of new formulations have never stopped in the history of epoxy resins. Since the discovery of diglycidyl ether of bisphenol A (DGEBA) by Schlack in 1934, numerous epoxy resins have been developed and commercialised, including both aromatic and cycloaliphatic monomers, as listed in Table 1. Generally, epoxy resins prepared from these monomers exhibit an amorphous structure without any local or global molecular order. While the properties of these resins can meet the requirements for most engineering applications, the increasing demand for high-performance materials, especially in the aerospace industry, has motivated scientists to search for advanced epoxy systems with superior properties.

Liquid crystalline epoxy networks

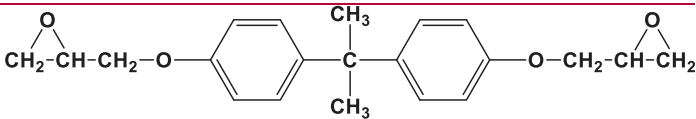
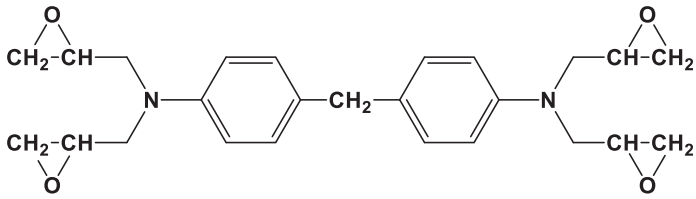
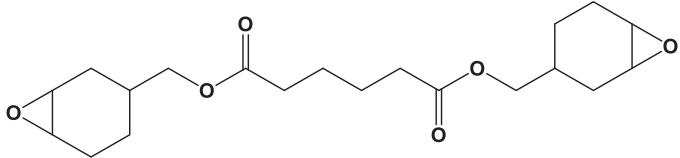
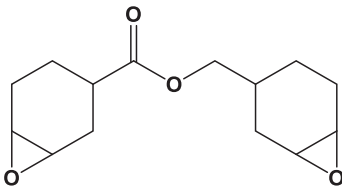
The successful commercialisation of high-performance liquid crystalline (LC) polymers such as Kevlar stimulated the interest in designing crosslinked LC materials. The prediction by de Gennes to develop liquid crystalline networks through the crosslinking reaction of reactive LC monomers resulted in the development of a group of materials known as liquid

CONTACT Yuzhan Li  yuzhanli@ustb.edu.cn  School of Materials Science and Engineering, University of Science and Technology Beijing, Beijing 100083, People's Republic of China; Buildings and Transportation Science Division, Oak Ridge National Laboratory, Oak Ridge, TN 37831, USA; Orlando Rios  orios1@utk.edu  Department of Materials Science and Engineering, The University of Tennessee, Knoxville, TN 37996, USA

© 2021 The Author(s). Published by Informa UK Limited, trading as Taylor & Francis Group

This is an Open Access article distributed under the terms of the Creative Commons Attribution License (<http://creativecommons.org/licenses/by/4.0/>), which permits unrestricted use, distribution, and reproduction in any medium, provided the original work is properly cited.

Table 1. Traditional aromatic and cycloaliphatic epoxy monomers.

Traditional epoxy monomer	Chemical structure
Diglycidyl ether of bisphenol A (DGEBA)	
Tetraglycidylmethylenedianiline (TGMDA)	
Bis[3,4-epoxycyclohexylmethyl] adipate (BECHMA)	
3,4-Epoxy cyclohexylmethyl 3,4-epoxycyclohexanecarboxylate (ECC)	

crystalline thermosets (LCTs) [5–7]. These materials combine the useful properties of liquid crystals (self-assembly, reversible phase transition, and macroscopic orientation) and thermosets (good thermal, mechanical, and barrier properties) [8]. A variety of LCTs were developed in the 1980s using monomers such as acrylate, methacrylate, epoxy, isocyanate, and maleimide [9]. Liquid crystalline epoxy networks (LCENs) have been among the most investigated LCTs because of their unique range of properties and potential applications [10]. Generally, LCENs are produced by the reaction between LC epoxy monomer and curing agent, resulting in a crosslinked network containing LC domains whose local and global order can be controlled during the curing reaction. These novel epoxy materials exhibit improved properties while maintaining the benefits of traditional epoxy resins, such as the richness of chemistry and ease of manufacturing. More importantly, the ability to modify the local and global order of the LC domains provides considerable design flexibility to further control the properties of the resins.

Early research of LCENs in the 1990s focused heavily on the synthesis of novel LC epoxy monomers [11,12], cure behaviour of these monomers with different curing agents [13–15], and characterisation of the fully cured resins [16–18]. Subsequent efforts in the 2000s were devoted to controlling the local and global order of the LC domains and understanding the reinforcing effects of these LC domains on fracture toughness [19–24], thermal conductivity

[25–27], and barrier properties of the LCENs [28–30]. Over the last decade, the design of LCENs with desired structures and properties has been the key focus area. Both lightly crosslinked (usually cured with difunctional carboxylic acids) and highly crosslinked (usually cured with tetrafunctional amines) LCENs have been synthesised and characterised.

In the lightly crosslinked system, the LC domains possess considerable flexibility. Therefore, they can show the general LC behaviour, such as reversible phase transition and macroscopic orientation. In contrast, in the highly crosslinked system, the LC domains and their local and global orientation are permanently frozen in the network. This difference has been used to generate LCENs with distinct properties and functionalities. The review article by Carfagna et al. provides excellent background information on both systems [10]. While highly crosslinked LCENs exhibit outstanding thermal and mechanical properties which make them ideal candidates for structural adhesives and conductive coatings [31], the tunable and adaptive performance of lightly crosslinked LCENs has resulted in an increasing interest over the past few years [32]. Combining breakthroughs in the field of dynamic covalent chemistry and liquid crystalline elastomers [33,34], Pei et al. developed lightly crosslinked LCENs exhibiting unprecedented capabilities [35]. This pioneering work has stimulated the development of LCENs with a variety of functionalities, including self-healing, shape-shifting, reprocessability, and recyclability. With recent progress in nanomaterials

and advanced manufacturing techniques, LCENs have emerged as a new platform for the development of functional materials and have shown great potential for a variety of applications, such as actuators, smart coatings and adhesives, tunable optical systems, and soft robotics.

In this article, we provide an overview of LCENs and their composites. The molecular engineering of LCENs, including the synthesis of monomers, selection of curing agents, and their unique curing behaviour, is discussed first. We then review approaches to control microstructure (local and global LC orientation) and properties of LCENs, highlighting some of their remarkable functionalities and applications enabled by these structure-processing-property relationships. Finally, we survey the forward-looking status of LCEN research in designing novel materials for future technologies.

Synthesis and molecular engineering

Like traditional epoxy resins, the versatility of LCENs originates from the wide variety of epoxy monomers and curing agents. The LC properties of fully cured LCENs are highly dependent on the monomers' molecular structure, although the selection of curing agents can be influential in some cases. In addition, the possibility of constructing LCENs using both step-growth and chain-growth polymerisation adds more flexibility to control their properties. This section reviews the synthesis of LC epoxy monomers and discusses the relationship between their molecular structure and LC properties. We also introduce the selection of curing agents and highlight the unique cure behaviour of LCENs.

Synthesis of epoxy monomer

General synthesis route

The synthesis of LC epoxy monomers shares a lot of similarities with that of traditional epoxy monomers. For example, Figure 1 shows two general routes for the synthesis of a biphenyl-based epoxy monomer (4,4'-Bis(2,3-epoxypropoxy)biphenyl, BP) that has been extensively used to produce LCENs. The monomer can be synthesised using a one-pot reaction between the corresponding diol and epichlorohydrin (EPI) in the presence of sodium hydroxide as a catalyst. While straightforward, this method requires a significant excess of epichlorohydrin to reduce side reactions, and the final product tends to contain a small number of oligomers. Alternatively, the monomer can be synthesised by converting the corresponding diol into a divinyl compound, followed by oxidation of the double bonds using peroxides such as meta-chloroperoxybenzoic acid (MCPBA). This approach allows for the preparation of LC epoxy monomers with high purity. However, two separate reactions are needed, and the purification of the final product is relatively complex. Liu et al. examined the synthesis of BP using both methods and found that the EPI route resulted in BP with a molecular weight distribution. In contrast, the MCPBA route resulted in BP with a distinct molecular weight [36]. In fact, both methods have been widely used to synthesise LC epoxy monomers with diverse structures and properties.

Molecular structure and geometry

Generally, LC epoxy monomer comprises rigid mesogens, flexible spacers, and reactive epoxy groups (Figure 2(a)). The arrangement of the three components can result in monomers with different

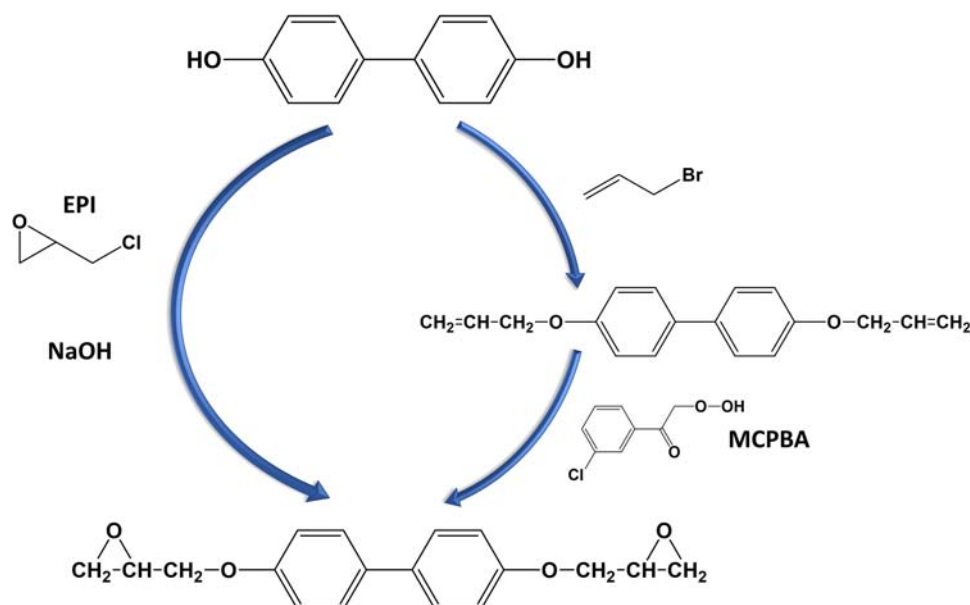


Figure 1. Available routes for the synthesis of a biphenyl-based LC epoxy monomer.

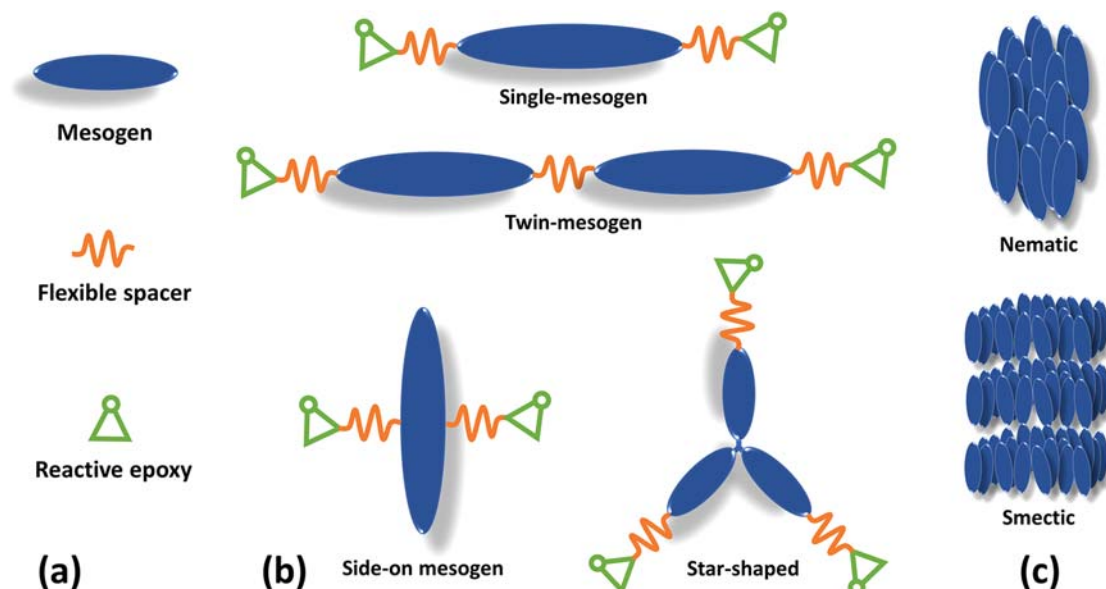


Figure 2. (a) Components of LC epoxy monomers, (b) typical structure and geometry of LC epoxy monomers, and (c) local molecular order of nematic and smectic LC phases.

geometries (Figure 2(b)). For a specific geometry, the LC monomer can be constructed using mesogens and flexible spacers with different molecular structures. These variables determine the monomer's thermal and LC properties, such as its phase transition temperatures and local molecular order (Figure 2(c)). For example, Table 2 shows three single-mesogen monomers constructed using different mesogens (biphenyl, methylstilbene, and phenyl benzoate), which exhibit distinct thermal and LC properties [37–39]. Because of this structure–property relationship, significant research on LCENs has focused on molecular engineering of the LC epoxy monomer.

Axial ratio and substitute

The design of LC epoxy monomers with proper dimensions is crucial to achieving desired thermal and LC properties. To elucidate the relationship between axial ratio and liquid crystallinity of LC epoxy monomers, Lee et al. synthesised a series of phenyl benzoate-based monomers and compared their thermal and LC behaviour [40]. They found that the LC phase became more stable as the monomers' axial ratio increased (Table 3). However, the increase of axial ratio required the construction of structures with more aromatic rings, which raised the melting temperature (T_m) of the monomers, leading to potential processing issues. For example, the T_m increased from 113°C for the mono-aromatic monomer to 192°C for the tetra-aromatic monomer.

To reduce the melting point of highly aromatic LC epoxy monomers, Lee et al. and Mormann et al. separately investigated the effect of substitution [41,42]. They both introduced a methyl group onto the central aromatic ring of a tri-aromatic epoxy monomer. As a


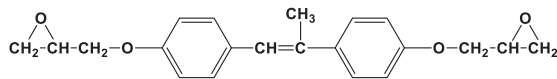
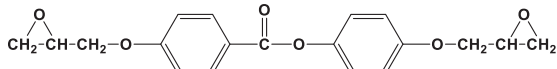
result, the T_m decreased from 183°C for the unsubstituted monomer to 131°C for the methyl substituted monomer (Table 4). The introduction of a chlorine substitute was not effective in reducing the T_m due to the increased polarity. In a subsequent work, Mormann et al. found that the introduction of bulky substitute such as methoxy can disrupt the self-assembly of mesogens, leading to a complete loss of liquid crystallinity of the monomer [43].

Flexible spacers

Modifying the flexible spacers is another way to tailor the thermal properties of LC epoxy monomers. Generally, increasing the length of flexible spacers results in decreased T_m and LC-isotropic phase transition temperature (T_i) of the monomer (Table 5, top) [44,45]. The reduction of T_i can be explained by the increased overall axial ratio of the monomer, which destabilises the LC phase. In addition to changing the length of flexible spacers, their position in the monomer has also been modified by many researchers, which has led to the development of twin-mesogen LC epoxy monomers [46]. These monomers consist of two mesogens connected through a flexible spacer. Choi et al. examined a series of azomethine-based twin LC epoxy monomers (Table 5, bottom) and observed an odd-even effect [47]. Monomers with even-numbered methylene units showed higher T_m and T_i values, which was ascribed to a well-organised packing structure.

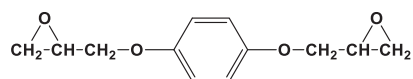
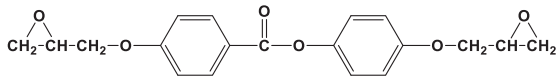
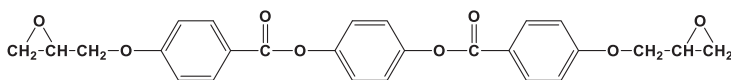
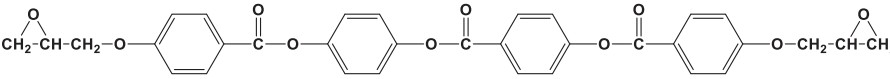
In summary, the extensive work on the molecular engineering of LC epoxy monomers greatly expanded the understanding of structure–property relationships. It provided valuable insights on designing monomers with suitable transition temperatures for the development of LCENs.

Table 2. Comparison of single-mesogen LC epoxy monomers with different mesogens.

Mesogen	LC epoxy monomer	Phase transition
Biphenyl	 4,4'-Bis(2,3-epoxypropoxy)biphenyl (BP)	^H Cr 156 I
Methylstilbene	 <i>p</i> -Bis(2,3-epoxypropoxy)- α -methylstilbene (DOMS)	^H Cr 124 I ^C I 109 N 62 Cr
Phenyl benzoate	 4-(2,3-Epoxypropoxy)phenyl 4-(2,3-epoxypropoxy)benzoate (PHBHQ)	^H Cr 119 I ^C I 93 N 79 Cr

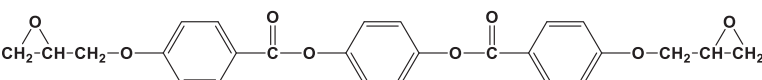
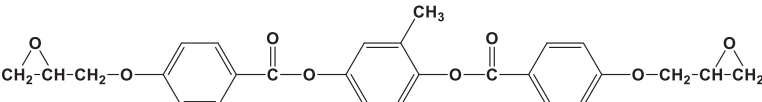
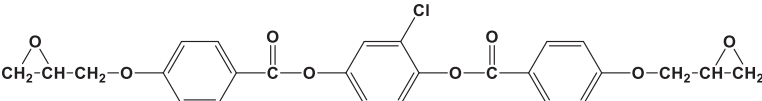
Notes: numbers indicate the phase transition temperatures and H, C, Cr, N, and I represent heating, cooling, crystalline, nematic, and isotropic, respectively. Phase transition data was collected from refs [15,37,38].

Table 3. Effect of axial ratio on the phase transitions of LC epoxy monomers.

LC epoxy monomer	Phase transition
	^H Cr 113 I
	^H Cr 116 I ^C I 93 N 79 Cr
	^H Cr 181 N 229 I
	^H Cr 192 N 271

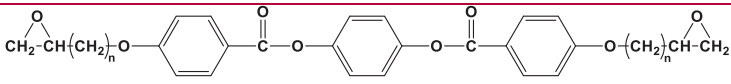
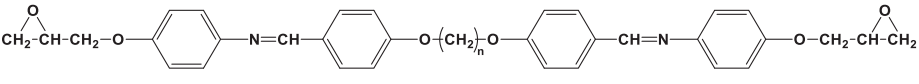
Notes: numbers indicate the phase transition temperatures and H, C, Cr, N, and I represent heating, cooling, crystalline, nematic, and isotropic, respectively. Phase transition data was collected from ref [40].

Table 4. Effect of substitute on the phase transitions of LC epoxy monomers.

LC epoxy monomer	Phase transition
	^H Cr 183 N 259 I
	^H Cr 131 N 223 I
	^H Cr 179 N 243 I

Notes: numbers indicate the phase transition temperatures and H, C, Cr, N, and I represent heating, cooling, crystalline, nematic, and isotropic, respectively. Phase transition data was collected from refs [41,42].

Table 5. Effect of flexible spacer on the phase transitions of LC epoxy monomers.

Single-mesogen LC epoxy monomer	<i>N</i>	Phase transition
	1	^H Cr 183 N 259 I
	4	^H Cr 119 N 213 I
	6	^H Cr 107 N 190 I
	9	^H Cr 110 N 165 I
Twin-mesogen LC epoxy monomer	<i>N</i>	Phase transition
	6	^H Cr 205 N 220 I
	7	^H Cr 165 N 181 I
	8	^H Cr 197 N 207 I
	9	^H Cr 160 N 177 I

Notes: numbers indicate the phase transition temperatures and H, C, Cr, N, and I represent heating, cooling, crystalline, nematic, and isotropic, respectively. Phase transition data was collected from refs [44–47].

Selection of curing agents

The strained ring structure provides epoxy with a high reactivity towards various curing agents, including amines, anhydrides, carboxylic acids, alcohols, and thiols. Because reactivity is not a constraint, curing agent selection is primarily based on the intended structures and properties of the final LCENs. Some frequently used curing agents for LCENs are summarised in Table 6. Generally, the use of coreactive curing agents results in a step-growth polymerisation, whereas the use of catalytic curing agents leads to a chain-growth polymerisation. The reaction mechanism of both processes has been covered in detail in the review articles by Pham et al. and Vidil et al. for traditional epoxy systems [1,2]. Here, we only highlight some special consideration when selecting curing agents for LCENs.

Coreactive, tetrafunctional

Aromatic diamines are the most frequently used coreactive curing agents for LCENs. The reaction proceeds through a step-growth process, starting with the formation of oligomers, followed by their crosslinking reaction. Since the formation of a LC phase is involved in the curing reaction, the timing of the crosslinking step becomes very important. Ideally, the crosslinking reaction should happen after a LC phase is formed through the self-assembly of oligomers. In this regard, the selection of curing agents greatly influences on the final structure of LCENs. As shown in Table 6, diamine curing agents can be categorised into symmetric and asymmetric based on their molecular structure. This is not usually a factor considered when curing traditional epoxy resins. However, in the case of LCENs, this symmetry factor strongly affects the step-growth process and therefore influences the LC phase formation [48,49]. For example, many researchers reported that when BP was cured with SAA, a smectic LCEN was obtained, whereas using DDS resulted in an amorphous resin [50,51]. The LC phase formation in BP-SAA was attributed to the asymmetric structure of SAA. Because of the two amine groups' unequal reactivity, the aromatic amine reacted first, resulting in linear

oligomers that were more likely to form a LC phase. The sulphonate amine reacted at a later stage, resulting in a delayed crosslinking reaction. In contrast, both amines groups in DDS reacted simultaneously and produced highly branched oligomers that cannot self-assemble into a LC phase, resulting in an amorphous resin. In summary, aromatic diamines are the primary choice when highly crosslinked LCENs are intended. The crosslinking networks can permanently fix any local or global LC order.

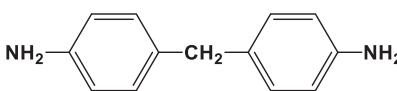
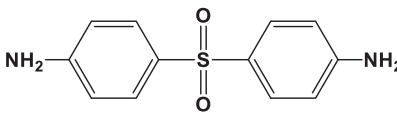
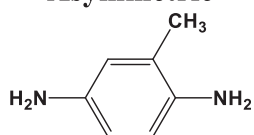
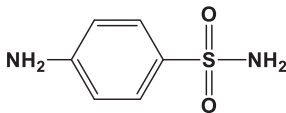
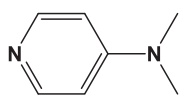
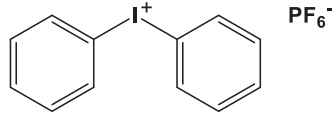
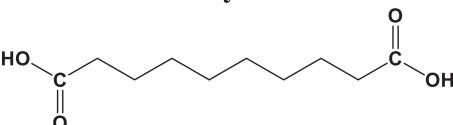
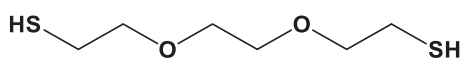
Catalytic

Highly crosslinked LCENs can be prepared using catalytic curing agents as well. Similar to the chain-growth polymerisation process of traditional epoxy resins, sulfonium and iodonium salts are used for cationic polymerisation, whereas tertiary amines and imidazoles are used for anionic polymerisation. The use of catalytic curing agents to produce LCENs has not received much attention. However, recently it has been shown that LCENs prepared using cationic polymerisation exhibited a highly ordered structure that resulted in improved thermal conductivity [52]. In addition, the photo-induced cationic polymerisation has shown great potential for additive manufacturing of LCENs because of its fast reaction kinetics and insensitivity to oxygen inhibition [53].

Coreactive, difunctional

Coreactive difunctional curing agents such as dicarboxylic acids and dithiols, are generally used for producing lightly crosslinked LCENs. The reaction follows the step-growth polymerisation mechanism. As the reaction proceeds, the oligomers are crosslinked through the hydroxyl groups generated in the ring-opening reaction of epoxy [54]. It is worth mentioning that the reaction between epoxy and thiol proceeds very fast and can be initiated by both heat and light, making it an attractive candidate for additive manufacturing where sufficiently high reaction speed and versatile initiation process are desired [55,56]. As mentioned earlier, the LC domains possess considerable flexibility in these lightly crosslinked networks and exhibit active responses to external

Table 6. Example of commonly used curing agents for LCENs.

Coreactive, tetrafunctional	
<p>Symmetric</p>  <p>4,4'-Methylenedianiline (MDA)</p>  <p>4,4'-Diaminodiphenyl sulfone (DDS)</p>	<p>Asymmetric</p>  <p>2,4-Diaminotoluene (DAT)</p>  <p>Sulfanilamide (SAA)</p>
Catalytic	
<p>Anionic</p>  <p>4-Dimethylaminopyridine (DMAP)</p>	<p>Cationic</p>  <p>Diphenyliodonium hexafluorophosphate (DPIHFP)</p>
Coreactive, difunctional	
<p>Carboxylic acid</p>  <p>Sebacic acid (SA)</p>	<p>Thiol</p>  <p>2,2'-(Ethylenedioxy)diethanethiol (EDDET)</p>

stimuli [57]. In particular, their ability to show reversible phase transition and macroscopic orientation after the crosslinking reaction has been used extensively for the design of shape memory materials.

In summary, the wide selection of curing agents and the diverse polymerisation pathways allow for the preparation of LCENs with well-controlled structures and properties. This has been the key advantage of LCENs over other LCTs, such as acrylate-based and polysiloxane-based systems. The detailed structure-processing-property relationships of LCENs will be discussed in Section 'Structure-processing-property relationships'.

Curing behaviour and reaction kinetics

As introduced in the previous section, the polymerisation process of LCENs depends on the choice of curing agent and mostly follows the mechanism observed for traditional epoxy resins. The majority of the curing studies of LCENs have focused on highly crosslinked systems cured with diamines. Here, we summarise

the main findings of these studies and highlight the unusual curing behaviour of LCENs caused by the LC phase formation.

The reaction between epoxy and amine involves several competing reactions, as shown in Figure 3 (a). The curing reaction starts with a nucleophilic attack of the primary amine to the electron-deficient carbon atom of epoxy, resulting in a secondary amine with a hydroxyl group. The secondary amine then reacts with another epoxy group, generating a tertiary amine with two hydroxyl groups. The reaction between secondary amine and epoxy is generally slower than that of primary amine due to steric hindrance effects. The hydroxyl groups formed in previous reactions can react with epoxy, which is responsible for the autocatalytic nature of the epoxy-amine reaction.

In the case of LCENs, the formation of LC phase introduces more complexity to the curing process [59,60]. Carfagna et al. first reported the unusual curing behaviour between DOMS and DAT

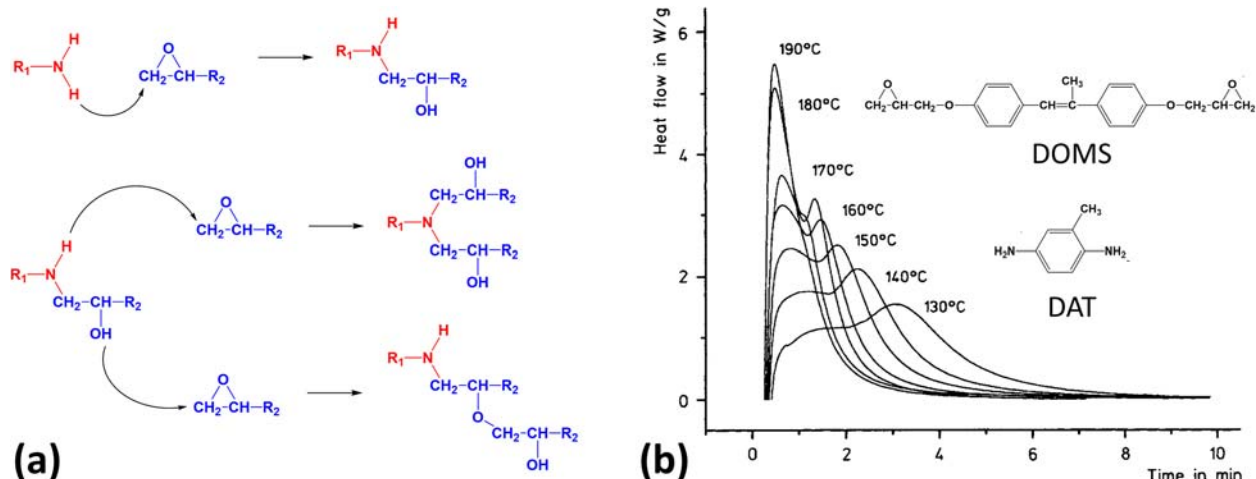


Figure 3. (a) Mechanism of epoxy-amine reaction and (b) isothermal DSC curing curves of a LCEN based on DOMS-DAT at different temperatures. Adapted with permission from ref [58]. Copyright 2003 John Wiley and Sons.

(Figure 3(b)) [37]. They performed a series of isothermal curing experiments using differential scanning calorimetry (DSC) and observed two exothermic peaks for the curing temperatures from 130°C to 170°C. However, for curing temperatures at 180°C and higher, only one exothermic peak was detected. The second exothermic peak was attributed to an acceleration of the curing reaction caused by the formation of a nematic LC phase. Similar behaviour has been reported for other LCENs as well. For example, Li et al. cured BP with SAA and found that when cured at temperatures below 200°C, the system formed a smectic LC phase, whose DSC curves exhibited two exothermic peaks (Figure 4(a)) [61]. Polarised optical microscopy (POM) experiment performed at 170°C confirmed that the second exothermic peak

was caused by the formation of the smectic phase (Figure 4(b)).

The unusual cure behaviour of LCENs has led to extensive research to understand their reaction kinetics. Following their initial report on the unusual cure behaviour of DOMS and DAT, Amendola et al. analysed the two exothermic peaks (Figure 3(b)) separately using an autocatalytic reaction model expressed by Equation (1):

$$\frac{d\alpha}{dt} = k \cdot f(\alpha) = A \cdot \exp\left(\frac{-E_a}{RT}\right) \cdot \alpha^m \cdot (1 - \alpha)^n \quad (1)$$

where $d\alpha/dt$ is the cure rate, k is kinetic constant, $f(\alpha)$ is the reaction model, A is the pre-exponential frequency factor, E_a is the activation energy, R is the gas constant, and T is the absolute temperature [58]. The activation energy associated with the two peaks

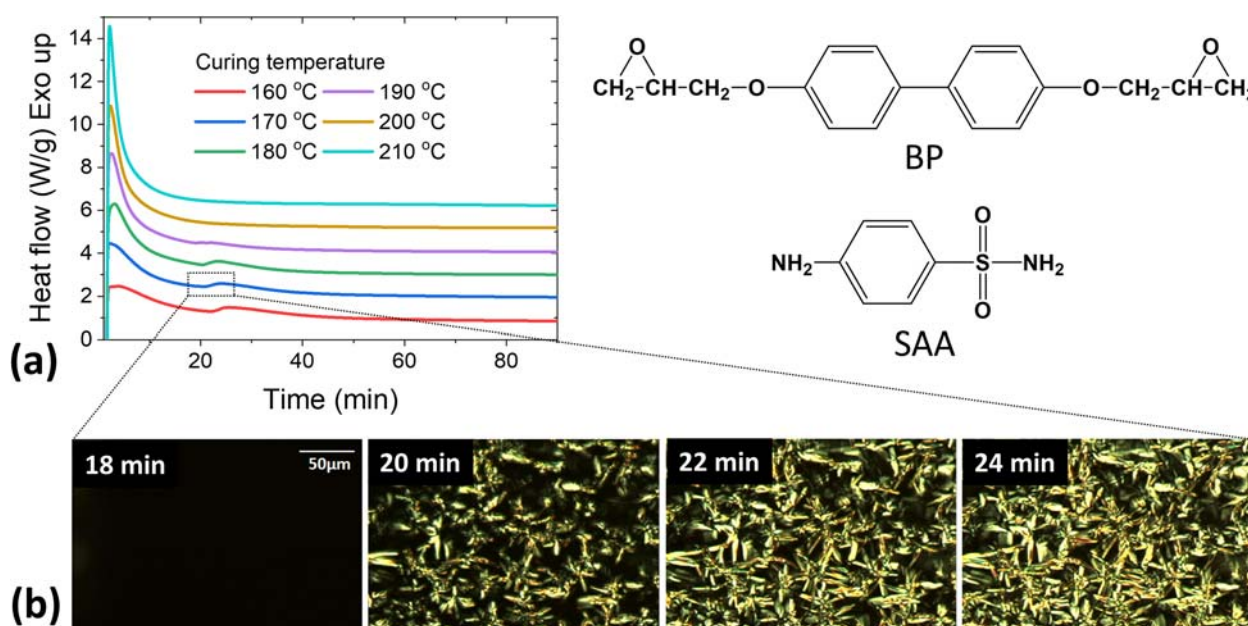


Figure 4. (a) Isothermal DSC curing curves of BP-SAA at different temperatures and (b) POM images captured at different reaction times at 170°C revealing the formation of a smectic LC phase. Adapted with permission from ref [61]. Copyright 2013 Elsevier.

was determined to be 35 and 42 kJ mol⁻¹, respectively. However, a significant increase of pre-exponential frequency factor by 26-fold was observed for the second peak, which resulted in a higher overall kinetic constant. The authors attributed this behaviour to the reduced viscosity due to the formation of the nematic phase. Similar kinetic analysis results were also obtained by Rosu et al. for the BP-SAA system [62]. It is worth mentioning that these studies used a pre-defined reaction model to fit the experimental data. While informative, these models are ineffective in describing the complex curing kinetics of LCENs. In this regard, Vyazovkin et al. developed a model-free isoconversional kinetic analysis method, in which a curing reaction can be modelled using multiple single-step kinetic equations, thereby enabling the correlation between the change of activation energy and the change of reaction mechanism [63]. In this method, dynamic DSC scans of different heating rates are used, and the reaction rate is directly related to the heat flow rate by Equations (2) and (3):

$$\frac{d\alpha}{dt} = \frac{dH/dt}{\Delta H} \quad (2)$$

$$\ln\left(\frac{d\alpha}{dt}\right)_{\alpha,i} = \ln(A_{\alpha}f(\alpha)) - \frac{E_{\alpha}}{RT_{\alpha,i}} \quad (3)$$

where $d\alpha/dt$ is the reaction rate, dH/dt is the heating heat, and H is total reaction heat. For a specific α at each heating rate β_i , the value of $(d\alpha/dt)_{\alpha,i}$ and $T_{\alpha,i}$ can be determined from DSC curves, and then the activation energy can be calculated from the plots of $\ln(d\alpha/dt)_{\alpha,i}$ vs $1/T_{\alpha,i}$ without using any reaction model [64]. Using this method, Li et al. investigated the cure kinetics of the BP-SAA system in detail [65]. In the experiment, LCENs were produced using low heating rates (1–4°C min⁻¹), whereas non-LCENs were produced using high heating rates (10–25°C min⁻¹), as shown in Figure 5(a,b). By comparing the two systems' activation energy, they found that the LC phase formation at the early stage of cure of LCEN facilitated the curing reaction, resulting in a decrease in activation energy (Figure 5(c)).

The use of advanced thermal analysis techniques, such as temperature modulated differential scanning calorimetry (TMDSC), has been proved effective in capturing the complex curing process of LCENs, as it allows for the deconvolution of overlapped thermal events. TMDSC experiment typically involves the application of a sinusoidal temperature oscillation to the traditional linear heating programme, thereby separating reversible and non-reversible heat flow signals. For example, Li et al. applied this technique on the BP-SAA system and captured an endothermic transition in the reversible heat flow signal, corresponding to the LC-isotropic phase transition [65]. However, in the total heat flow curve and the conventional DSC experiment, this process was not observed due to the overwhelming exothermic curing reaction. In a recent study, Mossety-Leszczak et al. observed that the curing enthalpy of a phenyl benzoate-based LCEN decreased with the increasing heating rate in conventional dynamic DSC experiments [66]. In order to elucidate this behaviour, the authors performed TMDSC and found an additional exothermic peak in the non-reversible heat flow curve, which was overshadowed by the reversible LC phase transition. This indicated that the exothermic curing process starts during the endothermic phase transition of the LC epoxy monomer. Although studies on the cure kinetics of LCENs have received less attention in recent years, they still play an important role in providing a fundamental understanding of the curing reaction of these novel epoxy systems.

Structure-processing-property relationships

The preparation of LCENs with desired structures, properties, and functions has been the key focus area. The structure-processing-property relationships have been investigated not only through the control of the molecular structure of LC epoxy monomers and curing agents but also through the control of local

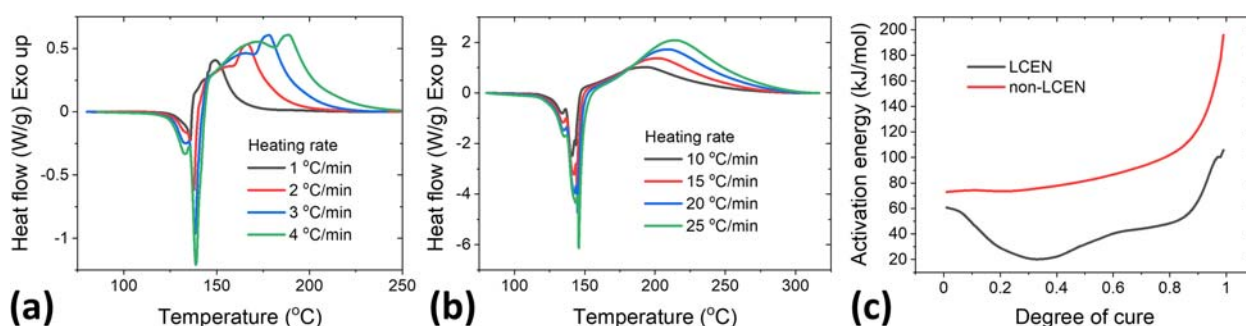


Figure 5. (a) Dynamic DSC curing curves of LCENs showing two exothermic peaks, (b) dynamic DSC curing curves of non-LCENs showing a single exothermic peak, and (c) evolution of activation energies of LCEN and non-LCEN determined using isoconversional kinetic analysis. Adapted with permission from ref [65]. Copyright 2014 Springer Nature.

and global order of the LC domains. In this section, we detail factors that influence the structures and properties of LCENs, including the choice of curing agents (reactivity and stoichiometry), polymerisation types (step-growth and chain-growth), and cure conditions (temperature and external field).

Control of network structure and local LC order

Network structure

As mentioned in Section ‘Selection of curing agents’, the selection of curing agent can result in LCENs with different network structures. This has been the primary strategy to control the performance of traditional epoxy resins. However, in the case of LCENs, the change of network structure also affects the flexibility of the LC domains, which determines their properties and functions. For example, in highly crosslinked LCENs, the LC domains are permanently fixed in the network, so they usually function as a reinforcing phase to improve mechanical and barrier properties because of their rigidity and ordered structure. On the other hand, in lightly crosslinked LCENs, the LC domains possess considerable flexibility to exhibit stimuli-responsive behaviour, which allows for the design of interesting functionalities, such as actuation and shape memory. Li et al. synthesised both highly and lightly crosslinked LCENs using the same biphenyl-based epoxy monomer (BP) [67]. The

former system was prepared using SAA as a curing agent (Figure 4(a)), whereas the latter system was produced using SA (Figure 6(a)). While both systems exhibited a layered smectic LC phase, they showed distinct properties (Table 7). It was found that the highly crosslinked LC domains in the BP-SAA system provided thermal and mechanical reinforcing effects, resulting in a material with high glass transition temperature (T_g), modulus, and creep resistance [68]. Conversely, the LC domains in the BP-SA system were flexible enough to show a temperature-induced reversible phase transition (Figure 6(b)) and a force-induced macroscopic LC orientation, confirmed by two-dimensional wide-angle X-ray scattering (Figure 6(c)). Taking advantage of these properties, thermally induced actuation behaviour of the LCEN was realised under a bias stress (Figure 6(d)). In addition, it was shown that the crosslink density and liquid crystallinity of the LCEN can be controlled by adjusting the molar ratio of BP and SA, which provided a simple way to further tailor the thermal and mechanical properties of the material (Table 7).

Local LC order and domain size

Generally, LCENs exhibit a polydomain structure when cured without any external field, in which the LC domains have random directions. Therefore, polydomain LCENs usually have isotropic properties. However, the LC domains may possess a specific

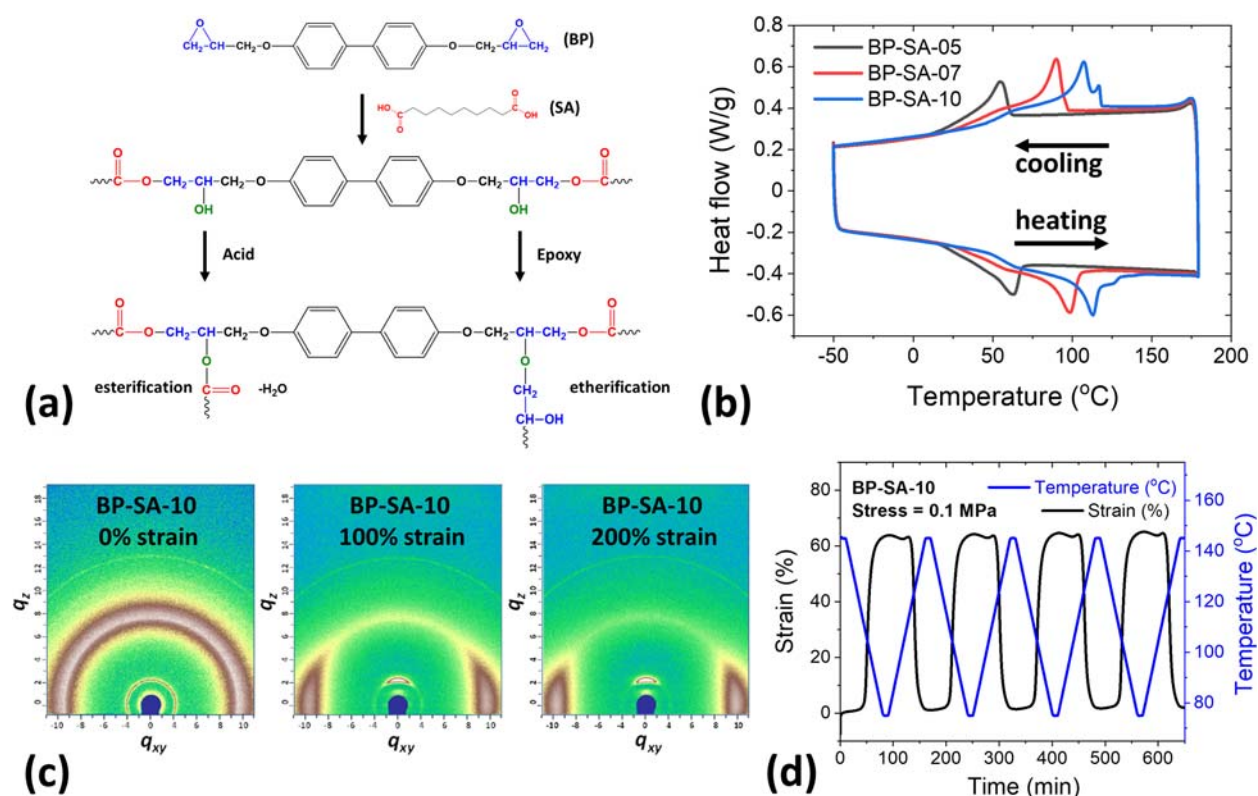


Figure 6. (a) Development of a lightly crosslinked LCEN using BP and SA, (b) temperature-induced reversible phase transition, (c) external force-induced macroscopic LC orientation, and (d) reversible actuation enabled by the stimuli-responsive behaviour of the LC domains. Adapted with permission from ref [67]. Copyright 2015 American Chemical Society.

Table 7. Thermal and mechanical properties of highly and lightly crosslinked LCENs prepared using the same epoxy monomer.^a

LCENs	Glassy modulus (GPa)	Rubbery modulus (MPa)	T_g (°C)	T_i (°C)
BP-SAA	3.98	270	190.8	N/A
BP-SA-05	2.38	3.94	28.8	54.9
BP-SA-07	2.26	2.14	44.0	92.5
BP-SA-10	2.45	1.62	57.2	112.8

^aAdapted with permission from ref [67]. Copyright 2015 American Chemical Society.

arrangement of mesogens, which is referred to as the local LC order, such as nematic and smectic (Figure 2(c)). This local molecular order affects the properties of LCENs and can be controlled by modifying the reaction conditions, such as the curing temperature and polymerisation type, which is usually not an option for traditional epoxy systems.

The curing temperature has been shown to strongly affect the local LC order of LCENs cured with diamines. This is related to the step-growth polymerisation process, in which the crosslinking step follows the chain-extension step. Since the self-assembly of mesogens in the chain-extension step is susceptible to temperature changes, it is possible to control the local LC order by adjusting the curing temperature. This local molecular order is then permanently fixed in the following crosslinking step. A detailed study was performed by Ortiz et al. who cured DOMS with MDA at different temperatures, which resulted in LCENs exhibiting isotropic, nematic, and smectic

local molecular order [19]. To elucidate the correlation between curing temperature and local LC order, they constructed a time-temperature-transformation diagram, as shown in Figure 7(a). The local molecular order difference resulted in materials with distinct fracture behaviour as revealed by a Chevron-notched three-point bending test. Interestingly, the presence of a smectic local order resulted in slow and stable crack propagation accompanied by exceptionally high fracture toughness of ($G_{Ic} = 1.62 \text{ kJ m}^{-2}$ and $K_{Ic} = 1.59 \text{ MPa m}^{1/2}$), whereas the presence of a nematic local order led to brittle failure with lower fracture toughness ($G_{Ic} = 0.75 \text{ m}^{-2}$ and $K_{Ic} = 1.46 \text{ MPa m}^{1/2}$), as shown in Figure 7(b,c), respectively. The high fracture toughness of the smectic LCEN was attributed to the isolated fracture of individual domains, which produced microscopic defects and voids near and around the crack tip. The triaxial stresses in neighbouring domains were relieved by this process, thus enabling substantial plastic deformation (Figure 7(d)). This reinforcing effect was not observed for the nematic LCEN because of the smaller size of the nematic domains. Inspired by this work, Harada et al. and Robinson et al. separately investigated the effect of LC domain size on the fracture behaviour of LCENs. Harada et al. produced azomethine-based, nematic LCENs with different domain sizes by varying the curing temperature [69]. It was found that higher curing temperatures led to faster curing rates and smaller nematic LC domains. The fracture behaviour was analysed using polarised

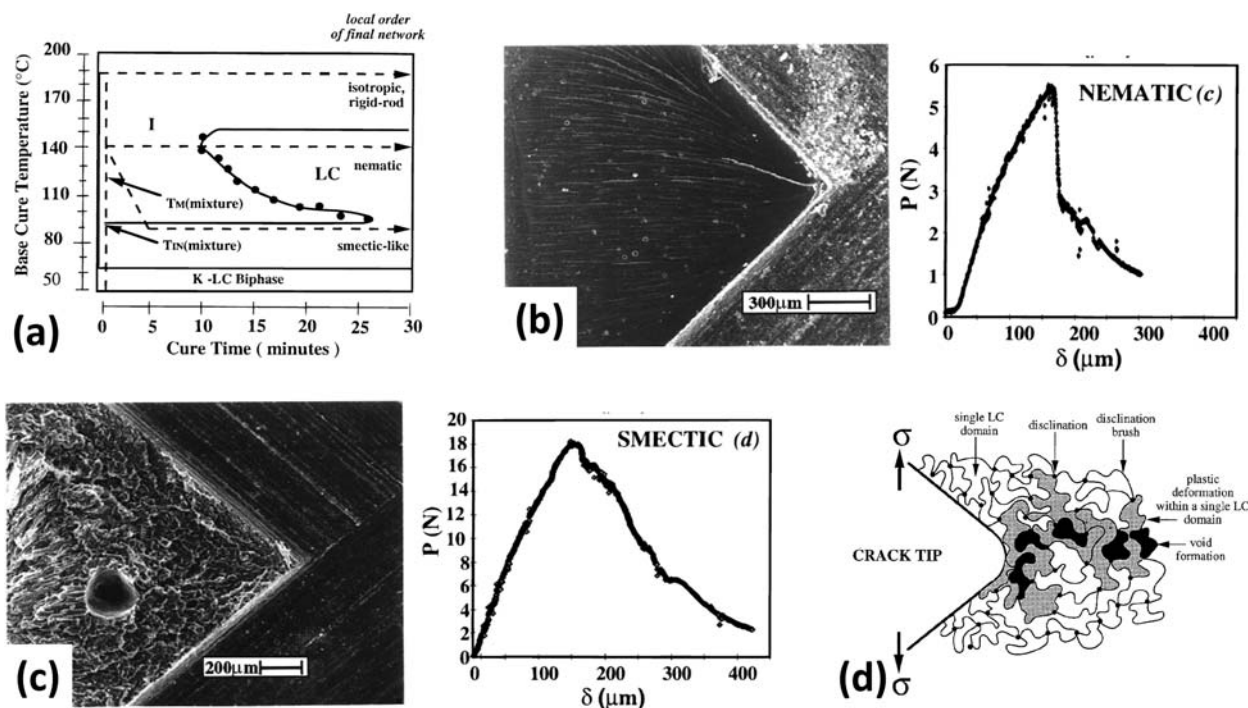


Figure 7. (a) Time-temperature-transformation diagram of DOMS-MDA elucidating the relationship between curing temperature and local molecular order, (b) brittle fracture behaviour of a nematic LCEN, (c) ductile fracture behaviour of a smectic LCEN, and (d) proposed fracture mechanism of the smectic LCEN. Adapted with permission from ref [19]. Copyright 1998 American Chemical Society.

infrared (IR) spectroscopy, which revealed that the cracks propagated through the amorphous region between LC domains. Larger LC domains were found to be more effective in deviating crack propagation, resulting in improved fracture toughness. Robinson et al. produced smectic LCENs with different domain sizes by changing the molar ratio of DOMS and SAA and found that the domain size decreased away from stoichiometry and resulted in a decrease of fracture toughness [70]. The size of LC domain also influences the dielectric properties of LCENs. For example, Guo et al. synthesised methyl and t-butyl substituted biphenyl epoxy monomers and cured them with DDM to produce LCENs with different domain sizes [71]. The methyl substituted LCENs exhibited a lower dielectric constant because of its larger domain size resulted from the well-packed mesogens.

Changing the polymerisation pathway is another method to control the local molecular order of LCENs. Castell et al. synthesised a series of azomethine-based LC epoxy monomers and investigated the curing behaviour of these monomers with DAT as a coreactive curing agent and with DMAP as a catalytic curing agent [72]. Interestingly, the use of DAT resulted in a nematic LCEN, whereas the use of DMAP resulted in a smectic LCEN. Similar behaviour was also reported by Ribera et al. on the curing of azomethine-based twin LC epoxy monomers [73]. The authors inferred that during the polymerisation the catalytic curing agent remained at the beginning of the propagating polymer chains and therefore facilitated the formation of highly ordered structures. Indeed, Islam et al. recently reported that the chain-

growth polymerisation of BP initiated by a cationic curing agent (N-benzyl pyrazinium hexafluoroantimonate, BPH) resulted in LCENs with a highly ordered microstructure due to linear weaving of the epoxy groups (Figure 8(a)) [52]. However, the use of a diamine curing agent (DDS) disturbed the molecular order of the mesogens, resulting in a less ordered microstructure. As shown in Figure 8(b), the sharp X-ray diffraction (XRD) peaks of BPH-cured LCEN indicated the presence of regular intersegmental spacing between the mesogens. It was also shown that the regulation of local molecular order reduced phonon scattering during heat transport, thereby improving the thermal conductivity of the resins from 0.34 W mK^{-1} for the DDS-cured to 0.48 W mK^{-1} for the BPH-cured, as shown in Figure 8(c).

Global LC order and advanced processing of LCENs

As discussed in Section ‘Control of network structure and local LC order’, modification of the local LC order is a simple and effective way to control the properties of LCENs. This flexibility can be further enhanced by applying external fields that induce a global LC order (macroscopic orientation). Enabled by the stimuli-responsive behaviour of liquid crystals, various methods can be used to induce a macroscopic orientation of LCENs, such as mechanical stretching [74,75], electric and magnetic field processing [76–80], surface orientation [81–84], and additive manufacturing [53]. Oriented LCENs often exhibit highly anisotropic optical, thermal, and mechanical properties.

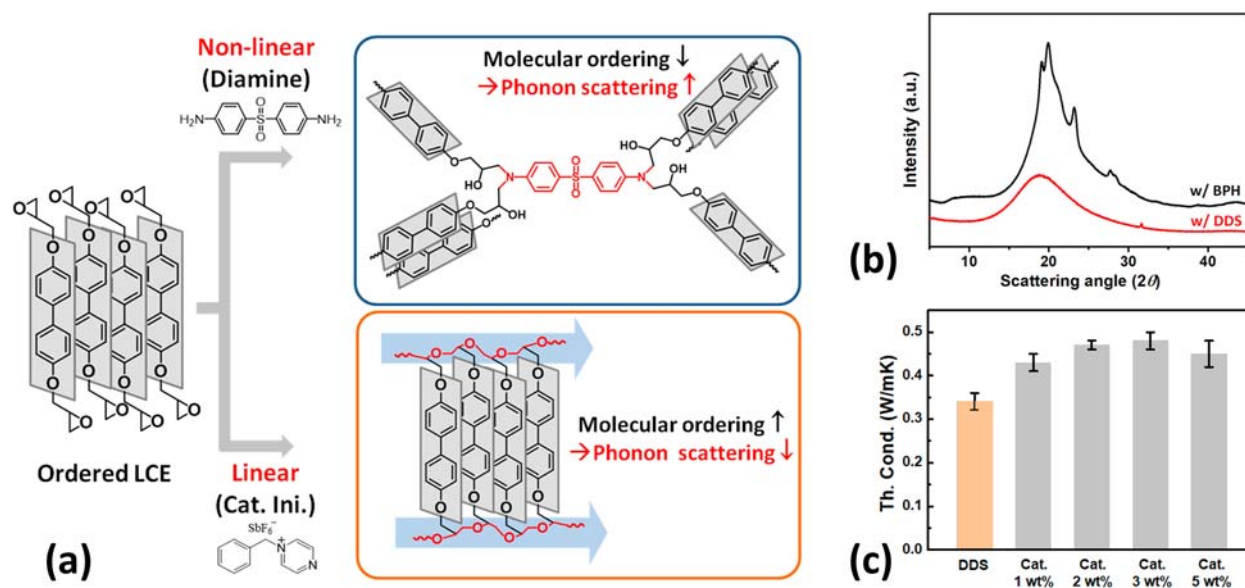


Figure 8. (a) Effect of polymerisation pathway on the local molecular order of biphenyl-based LCENs, (b) XRD spectra of the LCENs produced using step-growth and chain-growth polymerisation revealing the difference in microstructure, and (c) thermal conductivity of LCENs prepared using different polymerisation pathways. Adapted with permission from ref [52]. Copyright 2018 American Chemical Society.

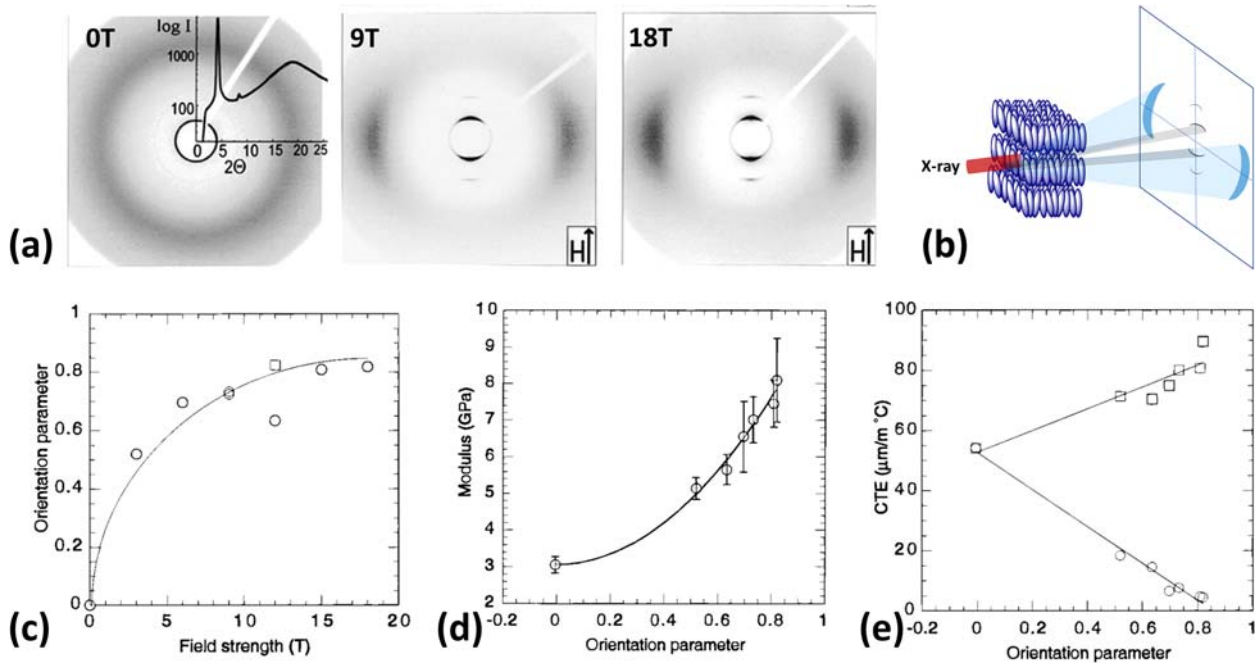


Figure 9. Magnetic field processing of LCENs based on DOMS-SAA: (a) WAXS patterns of the LCENs processed under different field strengths, (b) schematic illustration of WAXS of macroscopically oriented smectic LC domains, (c) effect of field strength on orientation parameter, (d) effect of macroscopic LC orientation on elastic modulus, and (e) effect of macroscopic LC orientation on CTE. Adapted with permission from ref [85]. Copyright 1998 American Chemical Society.

Magnetic field processing

Liquid crystals can be oriented in magnetic fields because of their anisotropic diamagnetic susceptibility. Many researchers have demonstrated the preparation of macroscopically oriented LCENs using magnetic field processing. Benicewicz et al. systematically investigated the effect of magnetic fields on the macroscopic orientation of LCENs prepared using DOMS and SAA [85]. The magnetic field application resulted in the alignment of mesogens along the direction of the applied field, which was then fixed by the crosslinking reaction. Two-dimensional WAXS patterns (Figure 9(a)) of fully cured LCENs confirmed the presence of smectic LC domains and their macroscopic orientation, as illustrated in Figure 9(b). Orientation parameters (S) were calculated from the inner scattering rings using Herman's method, as expressed in Equations (4) and (5), and were correlated with the field strength:

$$S = \frac{1}{2} (3\langle \cos^2 \alpha \rangle - 1) \quad (4)$$

$$\langle \cos^2 \alpha \rangle = \frac{\int_0^{\pi/2} I(\alpha) \cdot \sin \alpha \cdot \cos^2 \alpha \cdot d\alpha}{\int_0^{\pi/2} I(\alpha) \cdot \sin \alpha \cdot d\alpha} \quad (5)$$

where α is the angle between the smectic layer normal and the magnetic field, and $I(\alpha)$ is the intensity distribution calculated from the azimuthal intensity distribution. It was found that the orientation parameter reached a maximum value of approximately 0.8 at a field strength of 12 T (Figure 9(c)). The induced macroscopic LC orientation showed a

strong impact on the properties of the LCENs. For example, the elastic tensile modulus increased from 3.1 GPa for the unoriented sample to 8.1 GPa for the oriented sample cured at 18 T (Figure 9(d)). The influence of macroscopic LC orientation was also reflected by the LCENs' anisotropic coefficient of thermal expansion (CTE), as shown in Figure 9 (e). Following this work, Lincoln et al. statistically investigated the effects magnetic field strength, B-staging time, and curing time in the field on the LC orientation of the LCEN [79]. Both field strength and B-staging time were found to strongly affect the orientation process. For a given B-staging time, a field strength threshold was observed, which determined the occurrence of macroscopic LC orientation. A model was also constructed based on the statistical data, which allowed for predicting orientation parameter of the LCEN processed under different conditions. To further investigate the anisotropy of macroscopically oriented LCENs, Li et al. cured BP and SAA within a 9 T magnetic field and characterised the mechanical and thermo-mechanical properties of the resins using nanoindentation and thermomechanical analysis, respectively, as summarised in Table 8 [86].

Surface orientation

Surface orientation is another widely used method to align liquid crystals. As early as 1996, Amendola et al. demonstrated the possibility of producing macroscopically oriented LCEN films based on DOMS-DAT using surface orientation [82]. A planar

Table 8. Anisotropic properties of BP-SAA based LCENs after magnetic field processing.^a

	Contact stiffness ($\mu\text{N nm}^{-1}$)	Elastic modulus (GPa)	Hardness (GPa)	Average creep displacement (nm)	Glassy CTE ($\mu\text{m } ^\circ\text{C}^{-1}$)	Rubbery CTE ($\mu\text{m } ^\circ\text{C}^{-1}$)
Unoriented	34.3 ± 0.3	4.242 ± 0.064	0.242 ± 0.002	93.33 ± 1.14	66.75	126.9
Oriented, longitudinal direction	41.1 ± 1.3	5.284 ± 0.192	0.260 ± 0.009	88.66 ± 6.98	12.11	-27.44
Oriented, transverse direction	30.9 ± 0.7	3.669 ± 0.079	0.223 ± 0.009	115.10 ± 6.08	92.74	217.7

^aAdapted with permission from ref [86]. Copyright 2014 American Chemical Society.

orientation of the nematic LC domains was obtained using a rubbed polyimide layer, whereas a homeotropic orientation was achieved using a polysiloxane layer. The authors attributed this behaviour to the different polarity of the alignment layers, which resulted in different anchoring strengths for the mesogens. The designed orientation was preserved after the curing process and the oriented LCEN films exhibited strong birefringence. Recently, Tanaka et al. demonstrated the preparation of macroscopically oriented LCEN films using substrates with different surface free energy (γ) [83]. Low- γ substrate ($\sim 46 \text{ mN m}^{-1}$) was obtained through a thermal treatment at 250°C for 10 min in an atmosphere and high- γ substrate ($\sim 72 \text{ mN m}^{-1}$) was obtained through a UV/ozone treatment for 10 min after the thermal treatment. It was found that the low- γ substrate promoted a planar orientation of the mesogens.

In contrast, the high- γ substrate favoured a homeotropic orientation, confirmed by grazing incidence small-angle X-ray scattering (SAXS), as shown in Figure 10(a). Consequently, the LCEN films exhibited distinct thermal conductivity behaviour. An exceptionally high thermal conductivity of $5.8 \text{ W m}^{-1} \text{ K}^{-1}$ was observed for the homeotropically oriented LCEN film, whereas the film with a planar LC orientation showed a thermal conductivity of $0.4 \text{ W m}^{-1} \text{ K}^{-1}$. In subsequent work by the same authors, the effect of surface free energy on the LC orientation was further investigated using synchrotron radiation microbeam SAXS [84]. It was found that on a low- γ substrate the LCEN adopted a polydomain structure with a random orientation of the smectic domains, except at the droplet-air interface where a planar orientation was observed (Figure 10(b)). However, on a high- γ substrate, the LCEN adopted a

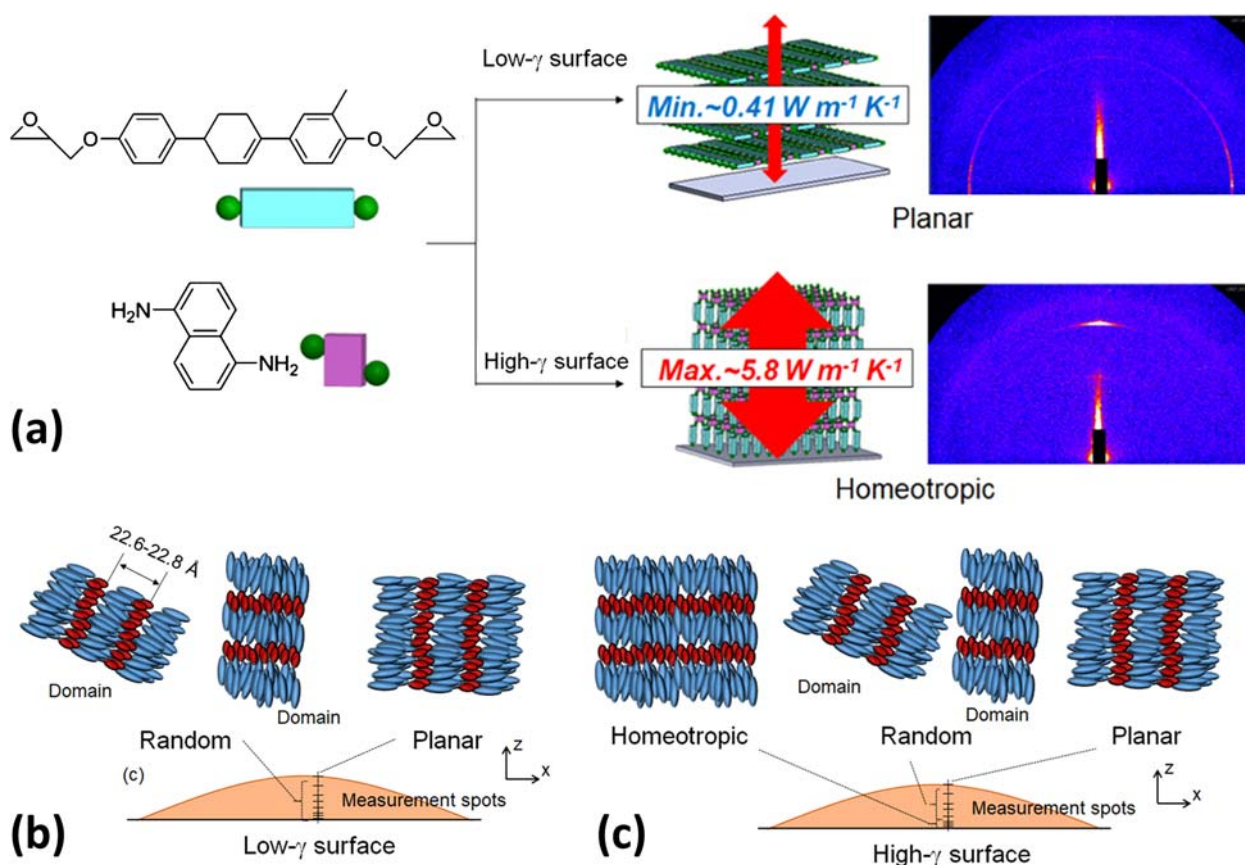


Figure 10. LCEN films with controlled global LC orientation and thermal conductivity: (a) effect of surface free energy of substrate on LC orientation, (b) orientation gradient of LCEN droplet on a low- γ substrate, and (c) orientation gradient of LCEN droplet on a high- γ substrate. Adapted with permission from refs [83,84]. Copyright 2018 and 2020 American Chemical Society.

homeotropic orientation in the vicinity (within 21 μm) of the substrate (Figure 10(c)). Therefore, when thin LCEN films were prepared on a high- γ substrate, homeotropically oriented LC domains were present throughout the film, resulting in a considerable increase of thermal conductivity. These films show potential applications, including conductive adhesives and thermal management coatings for electronic devices.

Additive manufacturing

In recent years, additive manufacturing (AM) has emerged as the leading technology to produce materials with controlled structures and geometries. The application of AM in the field of liquid crystalline networks has opened a whole new avenue for the control of LC orientation. The majority of the work has been focused on extrusion-based AM of acrylate-based LC systems [87–89]. As introduced in the pioneering work by Ambulo et al., the LC ink is subject to both shear and extensional flow during the extrusion AM process that results in macroscopic orientation of the LC domains [90]. The orientation can be fixed immediately using photopolymerisation after the ink is extruded, thereby allowing for the fabrication of materials with macroscopic and complex LC orientations. AM in LCENs is largely unexplored although the AM of traditional epoxy resins has been studied extensively. Recently, McCracken et al. demonstrated 2-photon direct laser writing (2P-DLW) for the development of oriented, microstructured LCENs, although the LC orientation was induced by surface orientation [53]. It was found that the robust cationic polymerisation of LCEN and its oxygen insensitivity suited well with the 2P-DLW process, through which diverse geometric arrays

with submicron resolution were generated (Figure 11 (a)). Interestingly, the authors demonstrated the fabrication of hybrid micro-actuators using orthogonal cationic polymerisation of LCEN and free radical polymerisation of LC acrylate (Figure 11(b)). Through the control of 2P-DLW micropatterned geometries which determined the LCEN density within the hybrid system, tunable actuation performance was realised, as shown in Figure 11(c).

LCEN composites

Polymer composites are hybrid materials consisting of a continuous polymer matrix with dispersed reinforcing fillers, and therefore combine the useful benefits of both components. The unique two-phase structure (amorphous and LC domains) of LCENs makes them attractive candidates as matrices for composite materials. Combining suitable fillers and LC domains can result in a synergistic effect, enabling remarkable improvement of properties [91–93]. In this section, we review different types of LCEN-based composites, emphasising the relationship between the nature and amounts of fillers and the curing behaviour, properties, and functionalities of the final composites.

Curing behaviour of LCEN composites

Most of the efforts on elucidating the effects of fillers on the cure kinetics of LCENs have been focused on diamine-cured systems. As early as 2002, the effect of different carbon fillers, namely carbon black (CB) and carbon nanotubes (CNTs), on the cure reaction of DOMS-SAA was investigated by Bae et al. [94]. The cure kinetics was monitored using dynamic DSC, and it was noticed that the addition of the

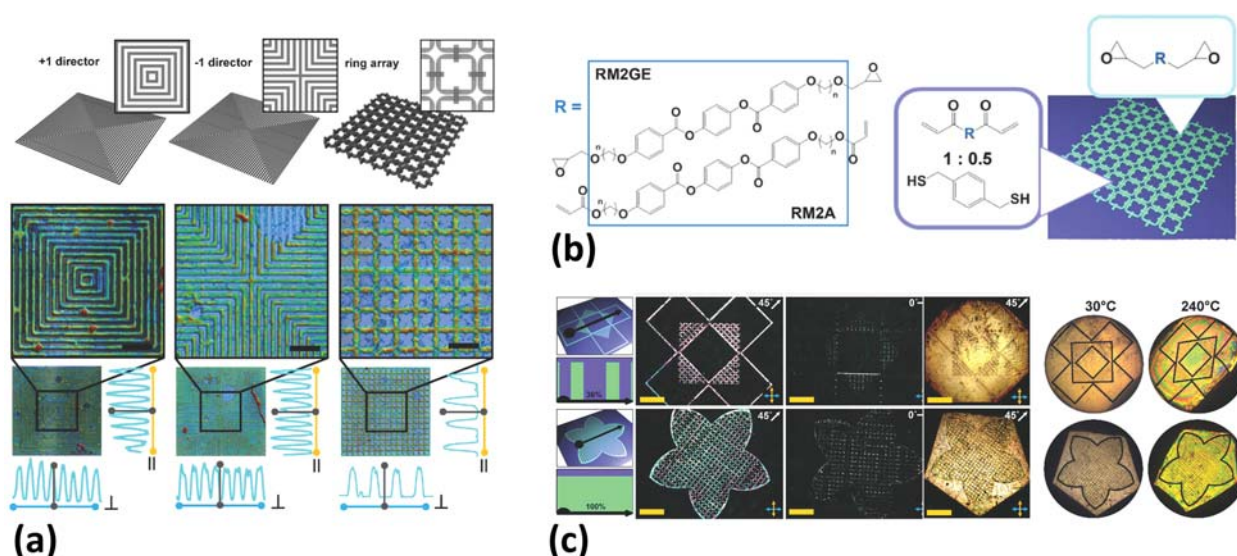


Figure 11. (a) Micropatterned LCEN arrays with submicron resolution enabled by 2P-DLW, (b) development of hybrid system consisting of LCEN and LC acrylate, and (c) 2P-DLW of hybrid microstructured actuators. Adapted with permission from ref [53]. Copyright 2019 John Wiley and Sons.

fillers retarded the cure reaction. The activation energies of the composites ($25.9 \text{ kcal mol}^{-1}$ for CB and $25.4 \text{ kcal mol}^{-1}$ for CNTs) were slightly higher than that of the neat LCEN ($25.1 \text{ kcal mol}^{-1}$). These outcomes were attributed to the steric restriction imposed by the carbon fillers on the nucleophile-electrophile interaction between amine and epoxy groups. In the same paper, it was also found that surface oxidation of the carbon fillers decreased the activation energy of the cure reaction by about $2.5 \text{ kcal mol}^{-1}$. Indeed, polar groups generated on the filler surface can act as nucleophiles, facilitating the opening of epoxy rings.

The effect of surface functionalisation was further investigated by Chen et al., who reported that the reaction rate of BP and DDS increased in the presence of BP-functionalised CNTs (Figure 12(a)) [95]. The activation energy of the composite decreased from 70.9 to 56.1 kJ mol^{-1} with a filler loading of $10 \text{ wt}\%$. Interestingly, the incorporation of thermal-insulating titanium dioxide (TiO_2) nanorods showed no effect on the activation energy, indicating that the high thermal conductivity of CNTs may play an important role in accelerating the cure reaction (Figure 12(b)). More recently, based on a BP-DDS system, Luo et al. synthesised a series of LCEN nanocomposites using pristine, acid-functionalised, and BP-functionalised nanodiamond (ND), as shown in Figure 12(c) [96]. It was found that the incorporation of ND accelerated the cure reaction regardless of the type of surface functionalisation, attributed to the unique structure of ND. However, BP-functionalised ND showed the lowest activation energy values due to the rigid structure of BP molecules (Figure 12(d)).

Besides carbonaceous particles, inorganic layered clays, such as montmorillonite (MMT), have been used as fillers in LCENs. Cai et al. found that MMT negatively affected the epoxy-amine reaction, lowering the reaction enthalpy and increasing the activation energies, especially at lower degrees of conversion [97]. It was found that the cation exchange reaction between amine and MMT caused the epoxy monomers to diffuse into the clay layers, contributing to the increased activation energy. The poor dispersion of MMT and the weak filler-matrix interaction was another reason, as evidenced also for conventional epoxy/MMT composites [98,99]. Therefore, organic intercalants have been used to improve the interfacial interaction between the nanoclay platelets and epoxy matrices. In this regard, Shen et al. elucidated the effect of three alkylammonium-based modifiers of MMT on the cure reaction between BP and SAA. All of them lowered the activation energy as they catalysed the epoxy ring-opening reaction [100].

Thermal conductivity of LCEN composites

In the field of electronics, heat dissipation represents a nodal issue affecting the performance of devices. Epoxy resins are frequently used as encapsulation materials. However, they show low values of thermal conductivity ($<0.3 \text{ W mK}^{-1}$). In this frame, LCENs have the potential to efficiently act as heat-dissipating materials as they exhibit thermal conductivity values as high as 0.89 W mK^{-1} [101,102] This is due to their anisotropic, highly oriented LC domains that promote heat transfer through a phonon vibration

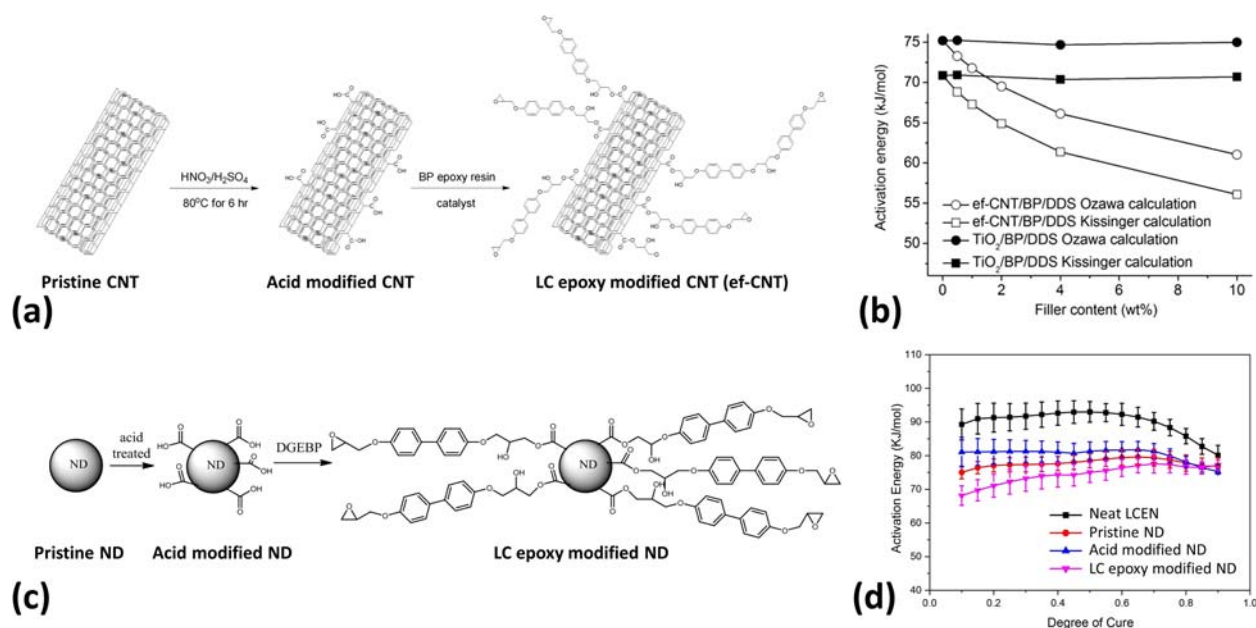


Figure 12. (a) Synthesis of LC epoxy functionalised carbon nanotubes (ef-CNTs), (b) effect of ef-CNTs and TiO_2 nanorods on activation energy of the cure reaction, (c) surface functionalization of ND, and (d) effect of ND and its surface functionalisation on activation energy of the cure reaction. Adapted with permission from refs [95,96]. Copyright 2010 John Wiley and Sons. Copyright 2018 Elsevier.

mechanism. By compounding with suitable fillers, further improvements of thermal conductivity of LCENs can be realised [103]. The nature, shape, size, and loading content of fillers are the key parameters controlling the thermal conductive properties of the composites.

Having a remarkably high thermal conductivity, boron nitride (BN) is one of the most employed additives. Harada et al. synthesised azomethine-based LCEN composites containing different amounts (up to 45 wt-%) of BN platelets and investigated the mutual interaction between the LC domains and the BN fillers [104]. They found that the local LC order had a significant influence on the dispersion of BN platelets (Figure 13(a)), which in turn affected their reinforcement efficiency. At a BN loading of 45 wt-%, the thermal conductivity of the smectic LCEN composite was 40% higher than that of the isotropic composite containing the same amount of BN (Figure 13(b)). This was related to the progressive BN platelets aggregation caused by the formation of the smectic LC domains (Figure 13(c)). Similar results were reported by Yang et al., who synthesised LCEN composites by curing BP with DDM in the presence of BN fillers [105]. The neat LCEN exhibited a high thermal conductivity of 0.51 W mK^{-1} because of the local nematic LC order (Figure 13(d)), which directed phonons to travel in the direction of the LC domains, thereby effectively

suppressing phonon scattering of the material (Figure 13(e)). When BN fillers were introduced to the material, the LCEN composite exhibited a high thermal conductivity of 1.02 W mK^{-1} at a 30 wt-% BN loading, twice as much as that of the DGEBA composite with the same BN loading (Figure 13(f)).

The influence of local LC order on the reinforcement efficiency of conductive fillers was also observed for alumina modified LCEN composites. Giang et al. synthesised a series of azomethine-based LCENs displaying smectic, nematic, and nematic-isotropic biphasic structures, and incorporated alumina conductive filler [106]. It was found that the thermal conductivity strongly depended on the local LC order of the LCEN. Indeed, at an alumina loading of 50 vol.%, thermal conductivity values of 2.83, 3.04, and 3.59 W mK^{-1} , were measured. Similar work has been carried out by Yeo et al., who systematically investigated various epoxy composites with alumina fillers [107]. They found that an ordered microstructure was crucial to achieving high thermal conductivity. In this regard, LCEN composites provided about 30% higher thermal conductivity than amorphous epoxy composites containing the same type and concentration of the conductive filler. A thermal conductivity value of 6.66 W mK^{-1} was observed for a BP-DDS system when 80 wt-% of alumina was incorporated.

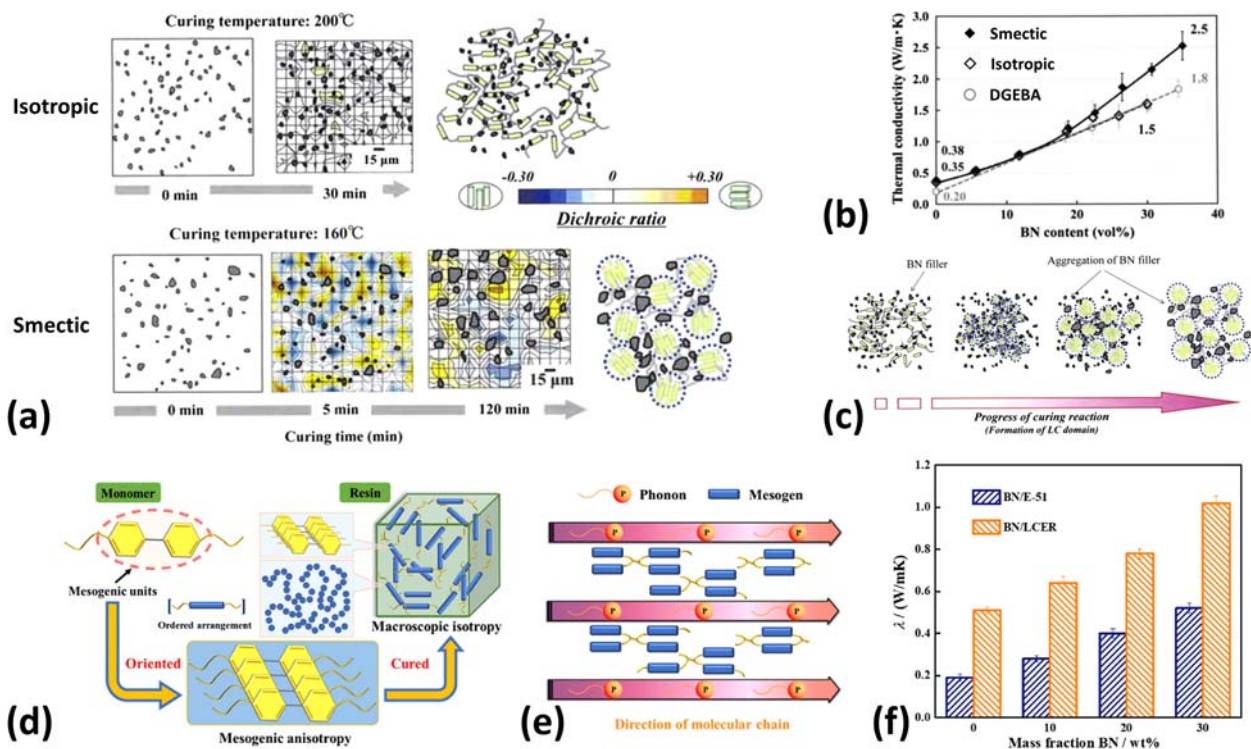


Figure 13. (a) Effect of local molecular order on the dispersion of BN platelets, (b) synergistic effect of local LC order and BN incorporation (c) schematic illustration of LC-assisted dispersion of BN platelets, (d) schematic illustration of microscopic anisotropy and macroscopic isotropy of a biphenyl LCEN, (e) regulated phonon transport through ordered LC domains, and (f) thermal conductivity of BN/LCEN and BN/DGEBA composites. Adapted with permission from refs [104,105]. Copyright 2013 and 2020 Elsevier.

Finally, remarkably high thermal conductivity values have been reported for graphene filled LCENs. Yeom et al. fabricated biphenyl-based LCEN composites containing graphene nanoplatelets (GNPs) [108]. To improve the filler-matrix interaction, a compatibiliser (BPIB) containing a biphenyl moiety and a pyrene moiety was synthesised and incorporated into the composites (Figure 14(a)). It was found that the use of BPIB significantly reduced the agglomeration of GNPs (Figure 14(b)) within the LCEN matrix because of the bridging effect of BPIB (Figure 14(c)). Through the modification of size, thickness, and dispersion of the GNPs, the authors reported an unprecedentedly high thermal conductivity value at a low filler content (44.9 W mK^{-1} at 13.6 vol.-%).

Thermal and mechanical properties of LCEN composites

Both fibres and nanoparticles have been used to improve the thermal and mechanical properties of LCENs. The first study on fibres-reinforced LCENs was reported by Carfagna et al. in 2000 based on a PHBHQ-DAT system containing 32 wt-% of carbon fibres [109,110]. Compared with a conventional DGEBA composite with the same amount of fibres, higher T_g values, fracture resistance, and elastic modulus were observed for the LCEN-based composite. In the same year, Sue et al. fabricated composites using

DOMS-SAA and revealed that the presence of carbon fibres promoted a preferred orientation of the LC domains along the fibre axis [111]. More recently, Guo et al. reported that the carbon fibre-induced LC orientation increased density of the LC domains and was responsible for the improved fracture toughness and thermal resistance [112].

In the past decade, more papers dealing with the fabrication of LCEN composites using nanoparticles have appeared in literature. Jang et al. reported the preparation of reinforced DOMA-SAA system using multi-walled carbon nanotubes (MWCNTs) and functionalised MWCNTs through surface oxidation [113]. The surface functionalisation was more effective in enhancing thermal and mechanical properties of the LCEN due to the interactions between the polar groups on the surface-modified nanotubes and the epoxy matrix. A drastic enhancement of thermal and mechanical properties was observed by Hsu et al. for BP-DDS based composites containing surface modified MWCNTs [114]. In this case, the nanotubes were oxidised first using a mixture of nitric acid and sulphuric acid, followed by attaching BP molecules onto the oxidised surface, which not only promoted the dispersion of nanotubes but also stabilised the LC domains. Consequently, the LCEN composites containing 2 wt-% of modified MWCNTs exhibited a T_g 70°C higher than that of the composite with pristine MWCNTs. Additionally, significant improvements on thermal stability, storage modulus, and

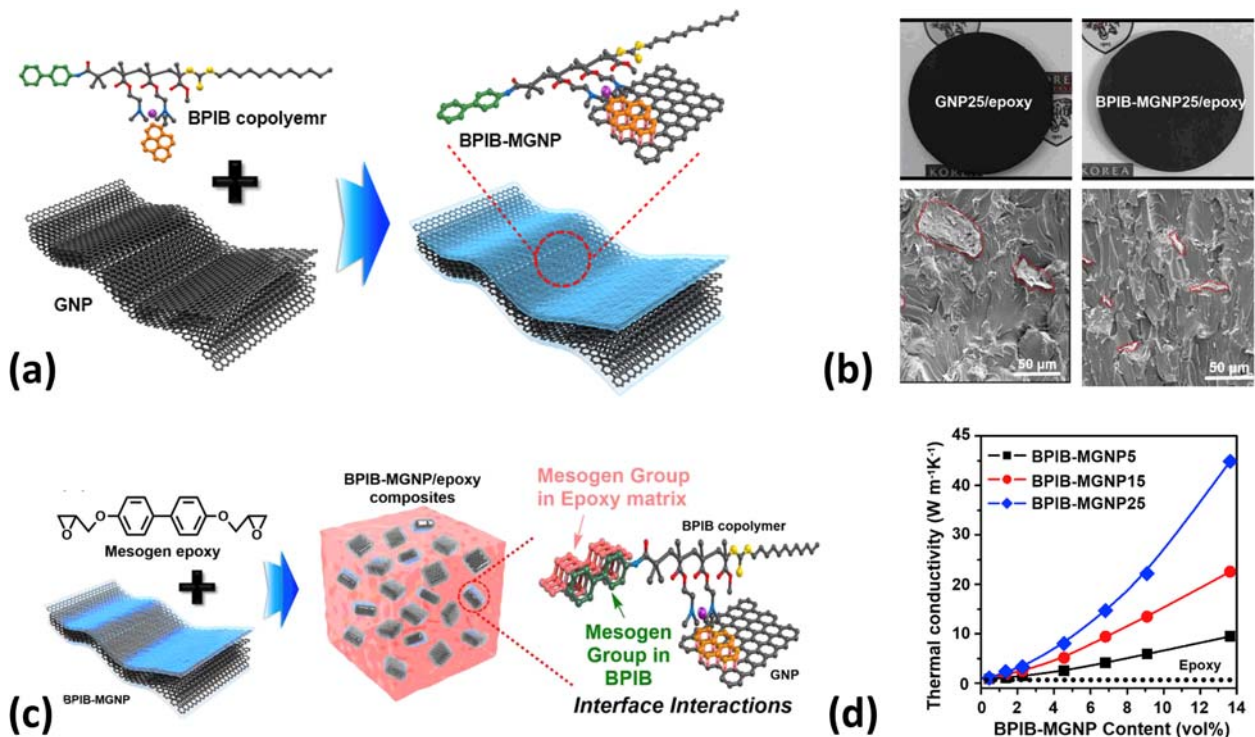


Figure 14. (a) Schematic illustration of the modification of GNPs using a compatibiliser BPIB, (b) SEM images of composites with unmodified and modified GNPs, (c) schematic illustration of the bridging effect of BPIB between the LCEN matrix and the GNP fillers, and (d) thermal conductivity of the interface-engineered composites as a function of GNP size. Adapted with permission from ref [108]. Copyright 2020 Elsevier.

hardness were observed and were attributed to the preferred orientation of the LC domains along the nanotubes.

Alumina and BN are the most used ceramic fillers to improve the thermal and mechanical properties of LCENs. In recent work by Lin et al., a detailed study on the effect of concentration and surface treatment (silane coupling) of BN fillers on the thermal and mechanical properties of a ketone-based LCEN was carried out [115]. Compared to the neat LCEN, the composite with 5 wt-% of modified BN exhibited an increase of storage modulus from 1968 to 2460 MPa and an increase of T_g from 228°C to 245°C. Moreover, the rubbery CTE reduced from 157 $\mu\text{m } ^\circ\text{C}^{-1}$ for the neat resin to 117 $\mu\text{m } ^\circ\text{C}^{-1}$ for the BN reinforced composite. Few studies have appeared so far on the influence of lamellar MMT on thermal and mechanical properties of LCENs. In their work, dating back to 2005, Ambrogi et al. investigated the properties of LCEN composites containing organophilic MMT [116]. The gained results evidenced that the T_g and the thermal decomposition temperature (T_d) decreased with increasing MMT loading, likely due to the homopolymerisation and plasticisation phenomena induced by the alkylammonium chains of MMT. Also, a significant reduction of tensile strength was observed for the composites. This has been related to the partial disruption of the LC structure due to the introduction of lamellar silicates.

Functionalities and applications

Owing to the unique structures and properties, LCENs exhibit various functionalities that cannot be offered by traditional epoxy resins. This section reviews some exciting functionalities reported in the literature for both highly crosslinked and lightly crosslinked LCEN systems and introduce the potential applications that these novel materials have enabled.

Highly crosslinked LCENs

As introduced in Section ‘Control of network structure and local LC order’, the diverse yet controllable LC order of LCENs is the key factor that differentiates them from traditional epoxy resins. This unique feature has allowed for the preparation of LCENs with highly tailorable thermal, barrier, and optical properties, enabling several novel applications [71,117,118].

For example, Jeong et al. explored the potential application of LCENs as lightweight, thermally conductive electronics packaging materials [119]. They synthesised a series of LCENs using cyanobiphenyl mesogens with epoxy side groups (Figure 15(a)) and found that the dipole–dipole and π – π

interactions between the cyanobiphenyl mesogens gave rise to a highly ordered structure that minimised phonon scattering during heat conduction (Figure 15(b)). As a result, the designed LCENs exhibited significantly higher thermal conductivity (0.46 W mK^{-1}) than that of traditional epoxy resins based on crystalline biphenyl and bisphenol A monomers (Figure 15(c)).

Nie et al., on the other hand, focused on the barrier properties of LCENs [121]. They investigated the water permeation behaviour of a LCEN based on DOMS-SAA and compared with that of an amorphous epoxy resin based on DGEBA-SAA. A significant reduction of water permeability was observed for the LCEN and was attributed to its ordered smectic structure, which formed a barrier limiting water transport pathways within the nanosized channels between the smectic layers. In addition, due to hydroxyl and amine groups in the channels, water transport was further reduced by the attractive forces exerted by these polar groups. The improved barrier performance of the LCEN, along with its outstanding thermal stability and adhesive properties, indicated that they could be used as protective coatings in next-generation electronic devices where excellent barrier properties and high flexibility are required. In another work, Kawamoto et al. showed that LCENs could be potentially used to fabricate composites for hydrogen storage systems [122]. They produced a series of LCENs using BP and DDM and evaluated their suitability as gas-barrier materials for type IV hydrogen storage vessels. In the experiment, the fabricated LCEN samples were exposed to hydrogen gas in a high-pressure vessel. The hydrogen content immediately after decompression was determined to be in the range of 403–1271 ppm, 25–75% lower than that of traditional DGEBA epoxy resins.

Shen et al. explored the potential use of LCENs as a novel stabilising phase for polymer-stabilised liquid crystals (PSLCs) [120,123,124]. In their work, PSLCs were fabricated through photopolymerisation a phenyl benzoate-based LCEN in LC solvents. The stabilising effect of the LCEN was evidenced by the highly oriented structure of the PSLCs when cured in a glass cell coated with rubbed polyimide layers (Figure 15(d), I and II). However, the use of DGEBA disrupted the initial orientation of the LC solvent molecules (Figure 15(d), III and IV), resulting in polymer-dispersed liquid crystal (PDLCs) with a porous, disordered network. The coupling of LCEN and LC solvent enabled a two-stage electro-optical performance of the PSLCs (Figure 15(e)). When the voltage of the applied electric field was lower than a critical value (V_c), the competition between the electric field effect and the anchoring effect of the LCEN framework disrupted the initial macroscopic orientation of the LC solvent molecules, leading to a reduction of transmittance. However,

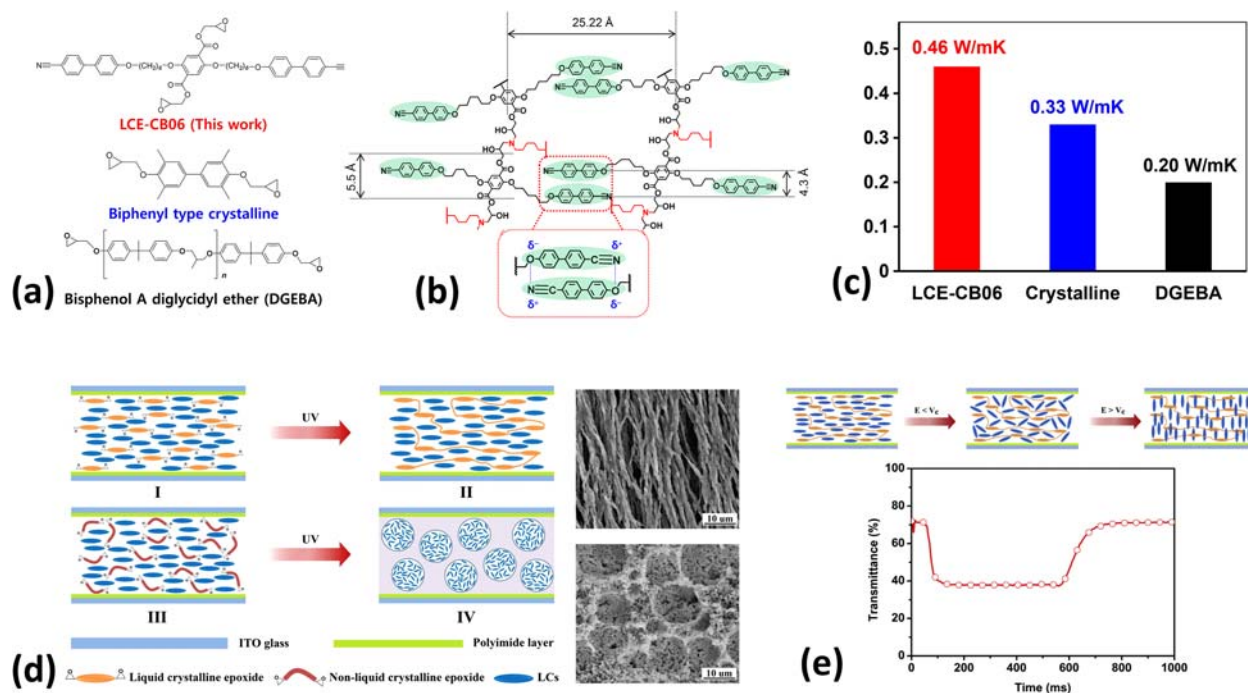


Figure 15. (a) Molecular structure of cyanobiphenyl, biphenyl, and bisphenol A epoxy monomers, (b) ordered microstructure of cyanobiphenyl-based LCEN enabled by the dipole-dipole and π - π interactions between the mesogens, (c) thermal conductivity of epoxy resins derived from different monomers, (d) comparison of PSLCs fabricated using a LCEN and PDLCs fabricated using a non-LC epoxy, and (e) two-stage electro-optical performance of PSLCs. Adapted with permission from refs [119,120]. Copyright 2018 John Wiley and Sons. Copyright 2019 Elsevier.

when the voltage was increased to a value higher than V_c , the electric field effect overpowered the anchoring effect, inducing a reorientation of the LC solvent molecules and resulting in an increase of transmittance. These novel PSLC materials have shown great potential for developing smart windows, electronic papers, and electrically tunable IR reflectors.

Some highly crosslinked LCENs also show promising biomedical applications. For example, Hsu et al. reported the potential use of LCEN nanocomposites as low-shrinkage dental restorative materials [125]. The nanocomposites were formulated using BP, a cycloaliphatic epoxy monomer (ECH), and silica nanoparticles. Cationic photopolymerisation of the mixture resulted in LCEN nanocomposites with excellent mechanical properties and extremely low post-gelation shrinkage, 50.6% less than that of commercial methacrylate-based composites. Cytotoxicity and biocompatibility of the LCEN nanocomposites were also evaluated and showed performance similar to that of commercial products, indicating that these nanocomposites are excellent candidates for dental restorative materials.

Lightly crosslinked LCENs

While the preparation of lightly crosslinked LCENs has been reported by Giamberini et al. as early as 1995 [126], these materials have not received much attention until the inspiring work by Pei et al. in

2014 [35]. Since then considerable progress has been made in the area and resulted in several smart materials with fascinating functionalities [127–134].

Pei et al. explored the potential applications of LCENs as actuators and shape memory materials. They designed and synthesised a lightly crosslinked LCEN vitrimer using BP as an epoxy monomer, SA as a difunctional curing agent, and 1,5,7-Triazabicyclo[4.4.0]dec-5-ene (TBD) as a transesterification catalyst (Figure 16(a)). Owing to the low crosslink density, the material exhibited a reversible LC-isotropic phase transition in addition to the glass transition. Using these two reversible thermal transitions, one-way, triple shape memory behaviour of the LCEN was realised (Figure 16(b)). More importantly, through the introduction of dynamic covalent bonds, the authors demonstrated the preparation of LCENs with exchangeable crosslinks, which allowed for easy processing and alignment (Figure 16(c)). Macroscopically oriented monodomain LCENs were readily produced using fully cured polydomain samples through the TBD-catalysed transesterification reaction. The prepared monodomain LCENs exhibited reversible and spontaneous thermal actuation enabled by the macroscopic orientation and reversible phase transition of the LC domains (Figure 16(d)). In addition, the simple alignment process allowed for the preparation of LCEN actuators with any shape, such as pin-shaped and dome-shaped actuators. These shapes are difficult to produce with the two-step alignment

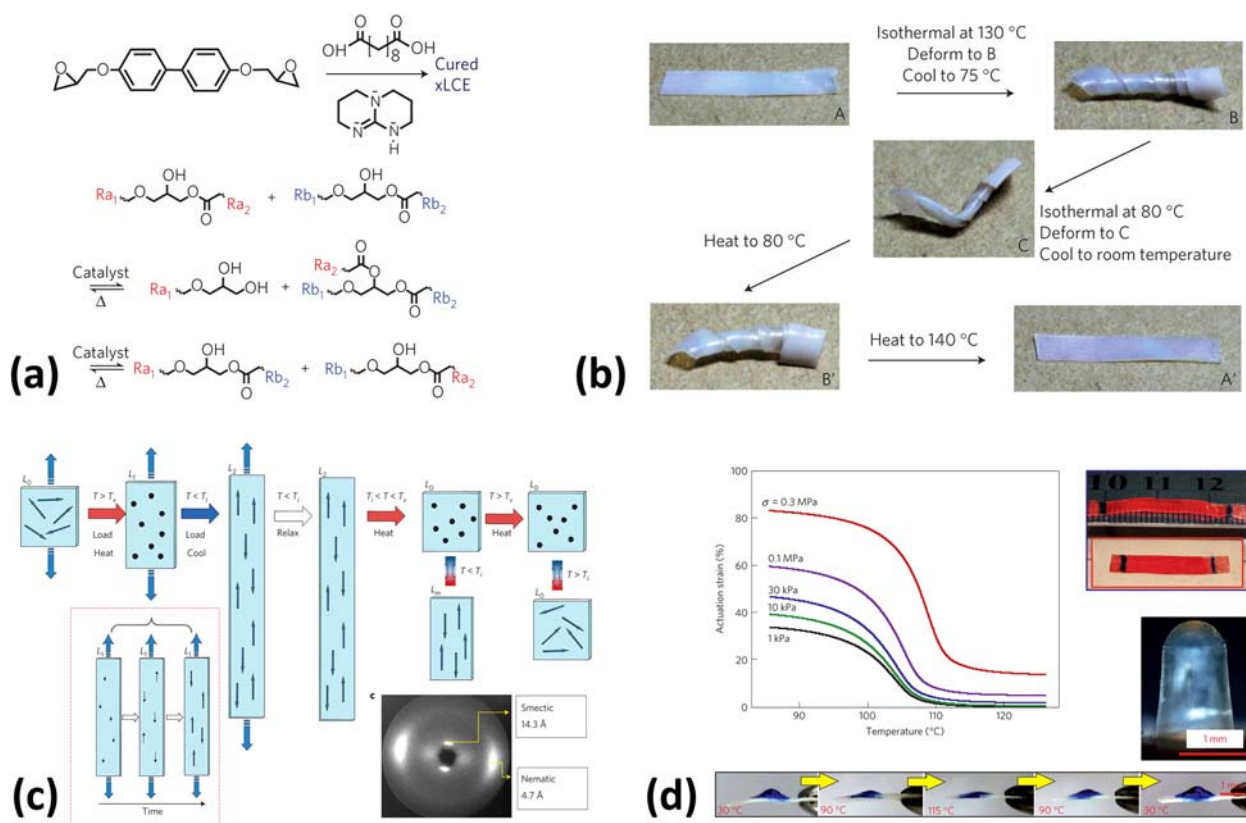


Figure 16. (a) Synthesis of LCEN vitrimer and TBD-catalysed transesterification between ester and hydroxyl groups, (b) one-way, triple shape memory behaviour of LCEN enabled by the reversible glass transition and LC phase transition, (c) post-synthesis alignment of LCEN vitrimer through transesterification, (d) thermal actuation of macroscopically aligned LCEN actuators with different shapes. Adapted with permission from ref [35]. Copyright 2013 Springer Nature.

process that are commonly applied in acrylate and polysiloxane-based liquid crystalline networks.

Following this pioneering work, many smart LCEN systems with novel functionalities have been reported. For example, Pei et al. developed multi-shape memory LCENs by joining epoxy vitrimers with different thermal transition temperatures (Figure 17(a)) [135]. The TBD-catalysed transesterification allowed the vitrimers to be welded via hot-pressing in any sequence, thereby enabling a stepwise shape recovery process of the hybrid LCEN films (Figure 17(b)). This approach dramatically simplifies the design of multi-shape memory polymers and enhances the ability to control the shape memory processes (shape programming and shape recovery). By selectively welding the three vitrimers, multi-shape memory behaviour of the hybrid LCEN films can be precisely controlled (Figure 17(c,d)).

To eliminate the processing restraints of LCEN vitrimers, such as moulding and hot-pressing, Yang et al. developed a light-assisted method, which enabled contactless processing and allowed for a spatial control of the LC order [136]. Through the incorporation of CNTs, they fabricated a LCEN composite whose transesterification reaction can be activated using IR lights because of the photothermal effect of CNTs (Figure 18(a)). Macroscopically aligned LCEN composites were

successfully prepared by shining lights on uniaxially stretched samples (Figure 18(b)). More importantly, they demonstrated that the degree of transesterification in the through-thickness direction of the LCEN composites can be controlled by tuning the intensity of the IR lights. This introduced an orientation gradient to the LCEN composites and enabled diverse actuation behaviour, such as contraction or bending (Figure 18(c)). Recently, using aligned CNT sheets, Wang et al. fabricated LCEN composites exhibiting electrically controlled actuation behaviour (Figure 18(d)) [137]. The aligned CNT sheets enabled Joule heating and acted as an important component introducing structural anisotropy to the composite film. Consequently, the composite film was able to show spontaneous bending behaviour powered by electricity without the need to induce macroscopic LC orientation (Figure 18(e)). The authors also demonstrated the potential use of the conductive LCEN composite as self-healing supercapacitors (Figure 18(f)).

In addition to enabling light and heat responsiveness, the incorporation of CNTs into LCENs has been shown to improve the fundamental shape memory performance. Lama et al. reported the synthesis of shape-memory LCEN composites filled with surface-modified MWCNTs [138]. They found that two-way actuation behaviour of the material under a uniaxial

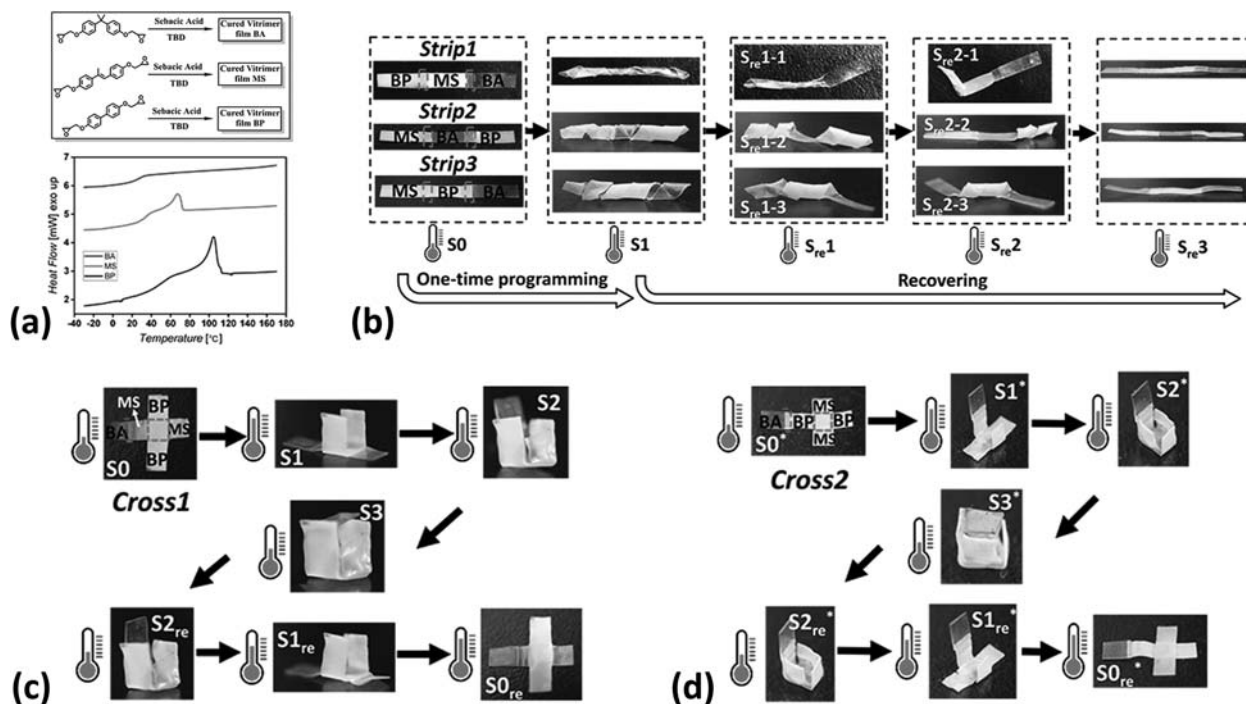


Figure 17. (a) Epoxy vitrimers with different thermal transition temperatures, (b) hybrid LCEN films consisting of vitrimers in different sequence that results in distinct shape recovery processes, (c) and (d) demonstration of hybrid LCEN films with controlled, multi-shape memory behaviour. Adapted with permission from ref [135]. Copyright 2015 John Wiley and Sons.

stress was significantly influenced by the presence of nanotubes. The neat LCEN showed a reversible actuation of about 20% upon thermal cycling (Figure 19(a)). In contrast, the composite containing the 0.75 wt-% of nanotubes exhibited a reversible actuation of about 75% under the same stress level (Figure 19(b)).

Moreover, the addition of MWCNTs greatly reduced the stress threshold required to initiate the shape change (Figure 19(c)). By investigating the microstructure evolution of the composite upon mechanical deformation, the authors revealed that the presence of MWCNTs reduced network rigidity of the LCEN,

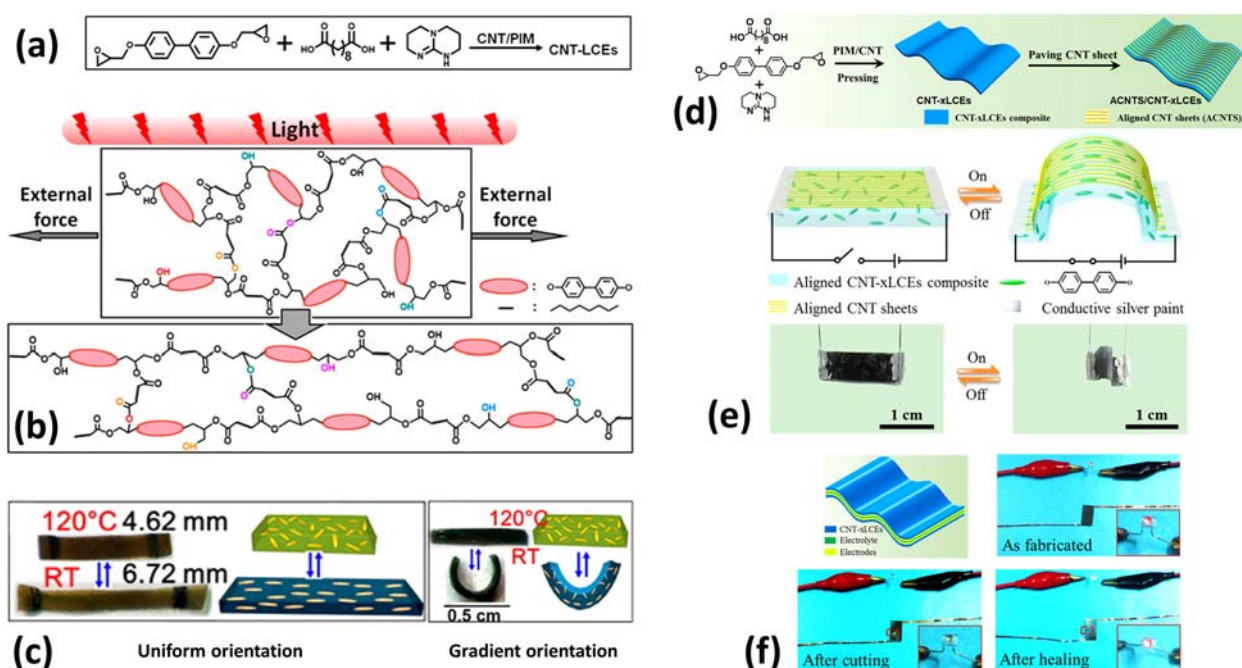


Figure 18. (a) Synthesis of CNT/LCEN composite, (b) light-triggered transesterification enabling contactless alignment of LCEN, (c) thermally-induced actuation behaviour of LCEN composites with different orientation gradients, (d) fabrication of aligned CNT sheets reinforced LCEN composite, (e) electrically powered actuation of CNT/LCEN composite, and (f) flexible LCEN composite supercapacitor with self-healing behaviour. Adapted with permission from refs [136,137]. Copyright 2016 and 2020 American Chemical Society.

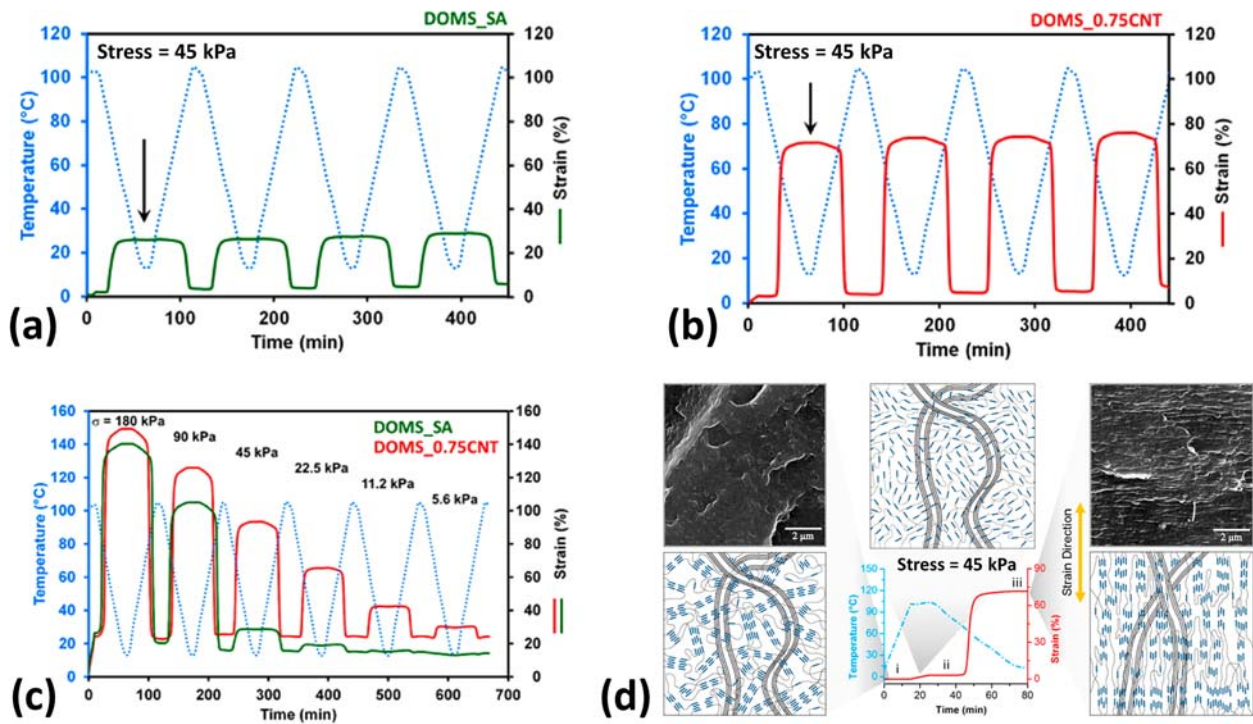


Figure 19. (a) Reversible actuation of neat LCEN under a uniaxial stress, (b) reversible actuation of MWCNT/LCEN composite under a uniaxial stress, (c) comparison of stress sensitivity of neat LCEN and the composite, (d) schematic representation of microstructure evolution of the LCEN composite during shape deformation. Adapted with permission from ref [138]. Copyright 2016 and 2020 American Chemical Society.

facilitating the polydomain-monodomain transition of the LC domains (Figure 19(d)). Similar results were also observed through the incorporation of graphene oxide [139].

Li et al. explored the possibility for the development of multi-functional LCENs [140]. They designed a simple approach that allowed for combining different functional building blocks, including azobenzene chromophores, liquid crystals, and dynamic ester bonds. An azobenzene-based epoxy monomer was polymerised with an aliphatic dicarboxylic acid to create exchangeable ester bonds that can be activated by a transesterification catalyst (Figure 20(a)). The LCEN exhibited various photo-induced bending behaviour enabled by the photoresponsive azobenzene molecules. For example, polarised blue light was used to control the macroscopic orientation of the azobenzene molecules on the light-fronting surface, which allowed for a bidirectional bending of the LCEN (Figure 20(b)). The use of polarised UV light also resulted in controlled bending behaviour of the LCEN but through a different mechanism. In this case, the polarised UV light triggered a trans-cis transformation of the azobenzene molecules on the light-fronting surface, generating contractive forces along the polarisation direction of the UV light and resulting in controlled bending behaviour (Figure 20(c)). The developed LCEN also exhibited light-induced triple shape memory behaviour owing to the photothermal

effect of the azobenzene molecules (Figure 20(d)). In addition, when combined with the dynamic ester bonds within the system, the photothermal effect allowed the LCEN to be repaired and reprocessed using UV light (Figure 20(e)).

To enhance the photoinduced mechanical force of photoresponsive LCENs, Lu et al. developed a strategy that exploited the mechanical strain energy of pre-stretched LCEN films (Figure 21(a)) [141]. Laminated films were prepared using pre-stretched LCEN film and biaxially oriented polypropylene (BOPP) film. By controlling the pre-strain of the LCEN film and architecture of the composite film, photoresponsive 3D objects with robust and continuous macroscopic motions were realised. For example, light-driven wheels and ribbons with controllable rolling speed and direction were developed using bilayer LCEN/BOPP composites (Figure 21(b)). The ability to precisely control the movement of these 3D objects allows for the design of soft robotics with more sophisticated motions. In subsequent work, the team incorporated gold nanorods (AuNR) into the LCEN, which enabled a near-infrared-light (NIR) responsiveness in addition to the UV-responsive behaviour of azobenzene (Figure 21(c)) [142]. When the researchers properly integrated the two mechanisms, a photo-operated robotic polymer crane was fabricated, capable of grasping, lifting, lowering down, and releasing an object (Figure 21(d)).

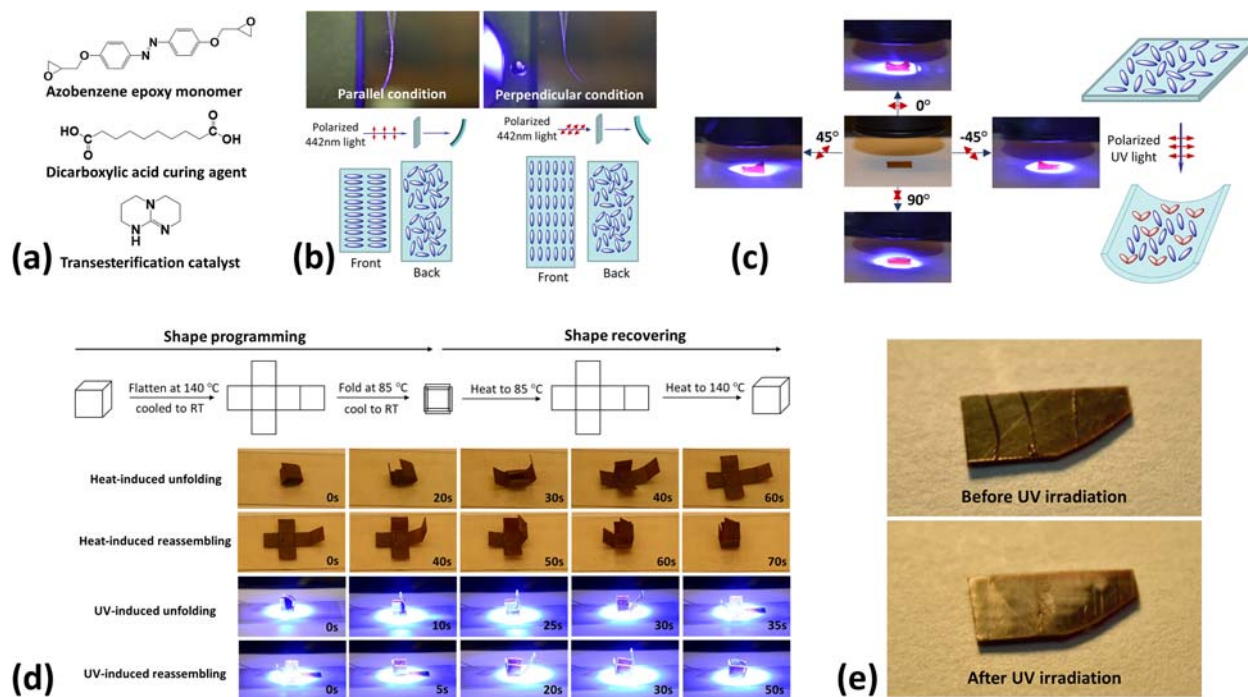


Figure 20. (a) Components of the preparation of multi-functional LCEN, (b) polarised blue light-induced bidirectional bending behaviour, (c) polarised UV light-induced controlled bending behaviour, (d) dual heat – and light-induced triple shape memory behaviour, (e) UV light-induced self-healing behaviour. Adapted with permission from ref [140]. Copyright 2016 American Chemical Society.

Conclusions and outlook

In the past few decades, remarkable advances have been made in the field of LCENs. While these materials were initially developed as a mechanically reinforced version of epoxy resins, continued research has revealed their huge potential by combining liquid crystals and epoxy networks. Compared to traditional epoxy resins, the presence of the LC domains provides considerable flexibility to tailor the properties of LCENs and enables novel

functionalities that are not offered by the conventional systems. Compared to other liquid crystalline networks, the versatile epoxy chemistry of LCENs allows for a greater control of the LC phase formation and network structures. This unique combination will continue to yield LCEN systems with novel structures and properties.

However, the successful preparation LCENs with desired functionalities will depend on the precise control of network structure and LC orientation, which

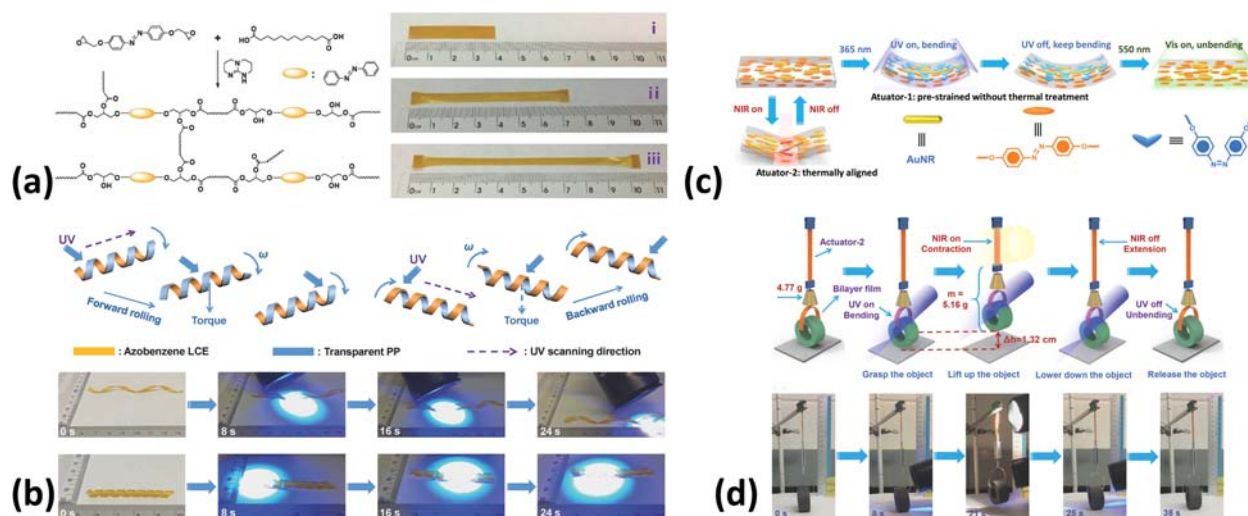


Figure 21. (a) Preparation of pre-stretched LCEN, (b) laminated LCEN/BOPP composite ribbons with controllable rolling speed and direction, (c) schematic illustration of two actuation mechanisms of AuNR/LCEN composites enabled by NIR and UV-vis lights, (d) light-controlled robotic crane fabricated through the integration of AuNR/LCEN composites with different actuation mechanisms. Adapted with permission from refs [141,142]. Copyright 2017 and 2018 John Wiley and Sons.

requires a rational selection of polymerisation pathways and processing techniques. While the step-growth polymerisation offers the possibility to tailor the LC phase formation of LCENs through the control of the chain growth process, effective methods are largely limited to the change of curing temperature or chemical reactivity of the monomers and curing agents. In this regard, the chain-growth polymerisation pathway represents a valuable option to control the overall reaction since both the initiation and propagation steps can be modified. The cationic polymerisation of LCENs, in particular, has shown great potential for the development of highly ordered LCENs with low cure shrinkage in an oxygen-rich environment and can be used in combination with acrylate-based systems to develop hybrid liquid crystalline networks. Concerning LC orientation control, additive manufacturing appears to be a powerful method to generate LCENs with macroscopic and programmed orientation. However, this area remains largely unexplored. The robust and versatile epoxy chemistry is expected to allow for the formulation of LC inks suitable for various printing techniques. In addition, the development of LCENs will continue to benefit from the progress in nanomaterials. While the use of traditional nanomaterials, such as CNTs and GNPs, have been found effective in improving the thermal and mechanical properties of LCENs, these improvements are far less ideal due to aggregation of the nanoparticles. Continued research on resolving the dispersion issues of nanoparticles and the exploration of novel fillers for LCENs, such as two-dimensional nanomaterials (graphene and MXenes), are needed to fully exploit the potential of LCEN composites. The challenge will be to properly integrate these tools to achieve the targeted structures and properties that can be translated into useful functionalities and applications. Another critical aspect to consider is the sustainability of LCENs. So far, scientific research has mainly addressed the preparation of LCENs with exchangeable crosslinks, which can be reused or recycled, thereby reducing waste disposal into the environment. In this respect, a remarkable advancement should encompass bio-based resources to provide novel functional LCEN epoxidised precursors, inline with the new international chemical regulations. This strategy will limit the consumption of non-renewable resources and CO₂ emissions, pushing academic and industrial actors to enhance circular economy models.

Acknowledgement

This work was sponsored by the U. S. Department of Energy's Building Technologies Office and Critical Materials Institute under Contract No. DE-AC05-00OR22725 with UT-Battelle, LLC.

Disclosure statement

No potential conflict of interest was reported by the author(s).

Funding

This work was sponsored by the U. S. Department of Energy's Building Technologies Office under Contract No. DE-AC05-00OR22725 with UT-Battelle, LLC.

ORCID

Yuzhan Li  <http://orcid.org/0000-0002-7432-2251>

References

- [1] Pham HQ, Marks MJ. Epoxy resins in Encyclopedia of Polymer Science and Technology. Fourth Edition. Edited by Herman F. Mark. New Jersey, John Wiley & Sons, Inc.; 2004, 678–804.
- [2] Vidil T, Tournilhac F, Musso S, et al. Control of reactions and network structures of epoxy thermosets. *Prog Polym Sci.* 2016;62:126–179.
- [3] Auvergne R, Caillol S, David G, et al. Biobased thermosetting epoxy: present and future. *Chem Rev.* 2014;114(2):1082–1115.
- [4] Jin FL, Li X, Park SJ. Synthesis and application of epoxy resins: a review. *J Ind Eng Chem.* 2015;29:1–11.
- [5] De Gennes PG. Possibilités offertes par la reticulation de polymeres en presence d'un cristal liquide. *Phys Lett A.* 1969;28(11):725–726.
- [6] Barclay GG, Ober CK. Liquid crystalline and rigid-rod networks. *Prog Polym Sci.* 1993;18(5):899–945.
- [7] White TJ, Broer DJ. Programmable and adaptive mechanics with liquid crystal polymer networks and elastomers. *Nat Mater.* 2015;14(11):1087–1098.
- [8] Douglas EP. Liquid crystalline thermosets in Encyclopedia of Polymer Science and Technology. Fourth Edition. Edited by Herman F. Mark. New Jersey, John Wiley & Sons, Inc.; 2002, 139–159.
- [9] Shiota A, Ober CK. Rigid rod and liquid crystalline thermosets. *Prog Polym Sci.* 1997;22(5):975–1000.
- [10] Carfagna C, Amendola E, Giamberini M. Liquid crystalline epoxy based thermosetting polymers. *Prog Polym Sci.* 1997;22(8):1607–1647.
- [11] Carfagna C, Amendola E, Giamberini M. Liquid crystalline epoxy resins containing binaphthyl group as rigid block with enhanced thermal stability. *Macromol Chem Phys.* 1994;195(7):2307–2315.
- [12] Carfagna C, Amendola E, Giamberini M, et al. Liquid-crystalline epoxy resins: a glycidyl-terminated benzaldehyde azine cured in the nematic phase. *Macromol Chem Phys.* 1994;195(1):279–287.
- [13] Lin QH, Yee AF, Earls JD, et al. Phase transformations of a liquid crystalline epoxy during curing. *Polymer (Guildf).* 1994;35(12):2679–2682.
- [14] Mormann W, Brocher M. Bröcher Markus Liquid crystalline thermosets (LCT) from diaromatic mesogenic diepoxides and aromatic diamines: synthesis and phase behaviour of model compounds and intermediate structures. *Polymer (Guildf).* 1998;39(25):6597–6603.
- [15] Giamberini M, Amendola E, Carfagna C. 1995. Liquid crystalline epoxy thermosets. *Mol Cryst Liq*

- Cryst Sci Technol Sect A-Mol Cryst Liq Cryst; 266:9–22.
- [16] Sue HJ, Earls JD, Hefner RE. *J Mater Sci.* 1997;32(15):4031–4037.
- [17] Lu MG, Shim MJ, Kim SW. Dielectric relaxation and mechanical properties of liquid crystalline epoxy thermosets. *J Appl Polym Sci.* 2000;77(7):1568–1573.
- [18] Lu MG, Shim MJ, Kim SW. Thermal degradation of LC epoxy thermosets. *J Appl Polym Sci.* 2000;75(12):1514–1521.
- [19] Ortiz C, Kim R, Rodighiero E, et al. Deformation of a polydomain, liquid crystalline epoxy-based thermoset. *Macromolecules.* 1998;31(13):4074–4088.
- [20] Ortiz C, Wagner M, Bhargava N, et al. Deformation of a polydomain, smectic liquid crystalline elastomer. *Macromolecules.* 1998;31(24):8531–8539.
- [21] Ortiz C, Belenky L, Ober CK, et al. *J Mater Sci.* 2000;35(8):2079–2086.
- [22] Harada M, Aoyama K, Ochi M. Fracture mechanism of liquid-crystalline epoxy resin systems with different phase structures. *J Polym Sci Part B-Polymer Phys.* 2004;42(22):4044–4052.
- [23] Harada M, Akamatsu N, Ochi M, et al. Tobita Masayuki investigation of fracture mechanism on liquid crystalline epoxy networks arranged by a magnetic field. *J Polym Sci Part B-Polymer Phys.* 2006;44(10):1406–1412.
- [24] Harada M, Sumitomo K, Nishimoto Y, et al. Ochi Mitsukazu relationship between fracture toughness and domain size of liquid-crystalline epoxy resins having polydomain structure. *J Polymer Sci Part B-Polymer Phys.* 2009;47(2):156–165.
- [25] Akatsuka M, Takezawa Y. Study of high thermal conductive epoxy resins containing controlled high-order structures. *J Appl Polym Sci.* 2003;89(9):2464–2467.
- [26] Harada M, Ochi M, Tobita M, et al. Thermal-conductivity properties of liquid-crystalline epoxy resin cured under a magnetic field. *J Polymer Sci Part B-Polymer Phys.* 2003;41(14):1739–1743.
- [27] Tokushige N, Mihara T, Koide N. Thermal properties and photo-polymerization of diepoxy monomers with mesogenic group. *Mol Cryst Liq Cryst.* 2005;428:33–47.
- [28] Lin CH, Huang JM, Wang CS. Synthesis, characterization and properties of tetramethyl stilbene-based epoxy resins for electronic encapsulation. *Polymer (Guildf).* 2002;43(10):2959–2967.
- [29] Feng JX, Berger KR, Douglas EP. Water vapor transport in liquid crystalline and non-liquid crystalline epoxies. *J Mater Sci.* 2004;39(10):3413–3423.
- [30] Giamberini M, Malucelli G, Ambrogi V, et al. The effect of chain packing on the thermal and dynamic mechanical behaviour of liquid-crystalline epoxy thermosets. *Polym Int.* 2010;59(10):1415–1421.
- [31] Kisiel M, Mossety-Leszczak B. *Eur Polym J.* 2020;124:109507.
- [32] Yang Y, Xu Y, Ji Y, et al. *Prog Mater Sci.* 2020;100710.
- [33] Montarnal D, Capelot M, Tournilhac F, et al. Silica-like malleable materials from permanent organic networks. *Science.* 2011;334(6058):965–968.
- [34] Ohm C, Brehmer M, Zentel R. Liquid crystalline Elastomers as actuators and sensors. *Adv Mater.* 2010;22(31):3366–3387.
- [35] Pei ZQ, Yang Y, Chen QM, et al. Mouldable liquid-crystalline elastomer actuators with exchangeable covalent bonds. *Nat Mater.* 2014;13(1):36–41.
- [36] Liu GD, Gao JG, Song LL, et al. Synthesis and curing of liquid-crystalline epoxy resins containing a biphenyl mesogen. *Macromol Chem Phys.* 2006;207(23):2222–2231.
- [37] Carfagna C, Amendola E, Giamberini M, et al. Curing kinetics of liquid-crystalline epoxy resins. *Liq Cryst.* 1993;13(4):571–584.
- [38] Barclay GG, Ober CK, Papatomas KI, et al. Liquid crystalline epoxy thermosets based on dihydroxymethylstilbene: synthesis and characterization. *J Polym Sci Part A – Polym Chem.* 1992;30(9):1831–1843.
- [39] Mormann W, Brocher M. “Liquid crystalline” thermosets from 4,4'-bis(2,3-epoxypropoxy)biphenyl and aromatic diamines. *Macromol Chem Phys.* 1996;197(6):1841–1851.
- [40] Lee JY, Jang JS. The effect of mesogenic length on the curing behavior and properties of liquid crystalline epoxy resins. *Polymer (Guildf).* 2006;47(9):3036–3042.
- [41] Lee JY, S J. Jang. Effect of substituents on the curing of liquid crystalline epoxy resin. *J Polym Sci Part A – Polym Chem.* 1998;36(6):911–917.
- [42] Mormann W, Brocher M. Liquid crystalline thermosets from triaromatic ester group containing diepoxides and aromatic diamines. *Macromol Chem Phys.* 1998;199(5):853–859.
- [43] Mormann W, Broche M, Schwarz P. Mesogenic azomethine based diepoxides – monomers for the synthesis of “liquid crystal” thermoset networks. *Macromol Chem Phys.* 1997;198(11):3615–3626.
- [44] Jahromi S, Lub J, Mol GN. Synthesis and photoinitiated polymerization of liquid crystalline diepoxides. *Polymer (Guildf).* 1994;35(3):622–629.
- [45] Mallon JJ, M P. Adams. Synthesis and characterization of novel epoxy monomers and liquid crystal thermosets. *J Polym Sci Part A – Polym Chem.* 1993;31(9):2249–2260.
- [46] Shiota A, K C. Ober. Synthesis and curing of novel LC twin epoxy monomers for liquid crystal thermosets. *J Polym Sci Part A – Polym Chem.* 1996;34(7):1291–1303.
- [47] Choi EJ, Ahn HK, Lee JK, et al. Liquid crystalline twin epoxy monomers based on azomethine mesogen: synthesis and curing with aromatic diamines. *Polymer (Guildf).* 2000;41(21):7617–7625.
- [48] Shiota A, Ober CK. Analysis of smectic structure formation in liquid crystalline thermosets. *Polymer (Guildf).* 1997;38(23):5857–5867.
- [49] Harada M, Ando J, Hattori S, et al. In-situ analysis of the structural formation process of liquid-crystalline epoxy thermosets by simultaneous SAXS/WAXS measurements using synchrotron radiation. *Polym J.* 2013;45(1):43–49.
- [50] Lee JY, Jang JS, Hwang SS, et al. Synthesis and curing of liquid crystalline epoxy resins based on 4,4'-biphenol. *Polymer (Guildf).* 1998;39(24):6121–6126.
- [51] Su WFA, Chen KC, Tseng SY. Effects of chemical structure changes on thermal, mechanical, and crystalline properties of rigid rod epoxy resins. *J Appl Polym Sci.* 2000;78(2):446–451.
- [52] Islam AM, Lim H, You NH, et al. Enhanced thermal conductivity of liquid crystalline epoxy resin using controlled linear polymerization. *ACS Macro Lett.* 2018;7(10):1180–1185.
- [53] McCracken JM, Tondiglia VP, Auguste AD, et al. *Adv Funct Mater.* 2019;29(40):10.

- [54] Ambrogio V, Giamberini M, Cerruti P, et al. Liquid crystalline elastomers based on diglycidyl terminated rigid monomers and aliphatic acids. Part 1. Synthesis and characterization. *Polymer (Guildf)*. 2005;46(7):2105–2121.
- [55] Stuparu MC, Khan A. Thiol-epoxy “click” chemistry: application in preparation and postpolymerization modification of polymers. *J Polym Sci Part A – Polym Chem*. 2016;54(19):3057–3070.
- [56] Gablier A, Saed MO, Terentjev EM. Transesterification in epoxy–thiol exchangeable liquid crystalline elastomers. *Macromolecules*. 2020;53(19):8642–8649.
- [57] Giamberini M, Cerruti P, Ambrogio V, et al. Liquid crystalline elastomers based on diglycidyl terminated rigid monomers and aliphatic acids. Part 2. Mechanical characterization. *Polymer (Guildf)*. 2005;46(21):9113–9125.
- [58] Amendola E, Carfagna C, Giamberini M, et al. Pisaniello Giuseppina curing reactions of a liquid crystalline epoxy resin based on the diglycidyl ether of 4,4′-dihydroxy- α -methylstilbene. *Macromol Chem Phys*. 1995;196(5):1577–1591.
- [59] Lin QH, Yee AF, Sue HJ, et al. Evolution of structure and properties of a liquid crystalline epoxy during curing. *J Polym Sci Part B-Polym Phys*. 1997;35(14):2363–2378.
- [60] Liu JP, Wang CC, Campbell GA, et al. Effects of liquid crystalline structure formation on the curing kinetics of an epoxy resin. *J Polym Sci Part A – Polym Chem*. 1997;35(6):1105–1124.
- [61] Li Y, Badrinarayanan P, Kessler MR. Liquid crystalline epoxy resin based on biphenyl mesogen: thermal characterization. *Polymer (Guildf)*. 2013;54(12):3017–3025.
- [62] Rosu D, Mititelu A, Cascaval CN. Cure kinetics of a liquid-crystalline epoxy resin studied by non-isothermal data. *Polym Test*. 2004;23(2):209–215.
- [63] Vyazovkin S, Mititelu A, Sbirrazzuoli N. Kinetics of epoxy–amine curing accompanied by the formation of liquid crystalline structure. *Macromol Rapid Commun*. 2003;24(18):1060–1065.
- [64] Vyazovkin S, Sbirrazzuoli N. Isoconversional kinetic analysis of thermally stimulated processes in polymers. *Macromol Rapid Commun*. 2006;27(18):1515–1532.
- [65] Li Y, Kessler MR. Cure kinetics of liquid crystalline epoxy resins based on biphenyl mesogen. *J Therm Anal Calorim*. 2014;117(1):481–488.
- [66] Mossety-Leszczak B, Kisiel M, Lechowicz JB, et al. Analysis of curing reaction of liquid-crystalline epoxy compositions by using temperature-modulated DSC TOPEM®. *J Therm Anal Calorim*. 2019;138(4):2435–2444.
- [67] Li Y, Pruitt C, Rios O, et al. Controlled shape memory behavior of a smectic main-chain liquid crystalline elastomer. *Macromolecules*. 2015;48(9):2864–2874.
- [68] Li Y, Kessler MR. Creep-resistant behavior of self-reinforcing liquid crystalline epoxy resins. *Polymer (Guildf)*. 2014;55(8):2021–2027.
- [69] Harada M, Okamoto N, Ochi M. Fracture toughness and fracture mechanism of liquid-crystalline epoxy resins with different polydomain structures. *J Polym Sci Part B-Polym Phys*. 2010;48(22):2337–2345.
- [70] Robinson EJ, Douglas EP, Mecholsky JJ. The effect of stoichiometry on the fracture toughness of a liquid crystalline epoxy. *Polym Eng Sci*. 2002;42(2):269–279.
- [71] Guo HL, Zheng J, Gan JQ, et al. Relationship between crosslinking structure and low dielectric constant of hydrophobic epoxies based on substituted biphenyl mesogenic units. *RSC Adv*. 2015;5(107):88014–88020.
- [72] Castell P, Galia M, Serra A. Synthesis of new epoxy liquid-crystalline monomers with Azo groups in the central mesogenic core. crosslinking with amines. *Macromol Chem Phys*. 2001;202(9):1649–1657.
- [73] Ribera D, Mantecon A, Serra A. Liquid crystalline thermosets from dimeric LC epoxy resins cured with primary and tertiary amines. *Macromol Symp*. 2003;199:267–276.
- [74] Barclay GG, McNamee SG, Ober CK, et al. The mechanical and magnetic alignment of liquid crystalline epoxy thermosets. *J Polym Sci Part A – Polym Chem*. 1992;30(9):1845–1853.
- [75] Giamberini M, Amendola E, Carfagna C. Lightly crosslinked liquid crystalline epoxy resins: The effect of rigid-rod length and applied stress on the state of order of the cured thermoset. *Macromol Chem Phys* 1997;198(10):3185–3196.
- [76] Li Y, Kessler MR. Liquid crystalline epoxy resin based on biphenyl mesogen: effect of magnetic field orientation during cure. *Polymer (Guildf)*. 2013;54(21):5741–5746.
- [77] Shiota A, Ober KC. Smectic networks obtained from twin LC epoxy monomers? Mechanical deformation of the smectic networks. *J Polym Sci Part B-Polym Phys*. 1998;36(1):31–38.
- [78] Tan CB, Sun H, Fung BM, et al. Properties of liquid crystal epoxy thermosets cured in a magnetic field. *Macromolecules*. 2000;33(17):6249–6254.
- [79] Lincoln DM, Douglas EP. Control of orientation in liquid crystalline epoxies via magnetic field processing. *Polym Eng Sci*. 1999;39(10):1903–1912.
- [80] Pottie L, Costa-Torro F, Tessier M, et al. Investigation of anisotropic epoxy–amine thermosets synthesised in a magnetic field. *Liq Cryst*. 2008;35(8):913–924.
- [81] Lee JY. Relationship between anisotropic orientation and curing of liquid crystalline epoxy resin. *J Appl Polym Sci*. 2006;102(2):1712–1716.
- [82] Amendola E, Carfagna C, Giamberini M, et al. Anisotropic liquid crystalline epoxy thermoset. *Liq Cryst*. 1996;21(3):317–325.
- [83] Tanaka S, Hojo F, Takezawa Y, et al. Highly oriented liquid crystalline epoxy film: robust high thermal-conductive ability. *ACS Omega*. 2018;3(3):3562–3570.
- [84] Tanaka S, Takezawa Y, Kanie K, et al. Muramatsu Atsushi homeotropically aligned monodomain-like smectic-A structure in liquid crystalline epoxy films: analysis of the local ordering structure by microbeam small-angle X-ray scattering. *ACS Omega*. 2020;5(33):20792–20799.
- [85] Benicewicz BC, Smith ME, Earls JD, et al. Magnetic field orientation of liquid crystalline epoxy thermosets. *Macromolecules*. 1998;31(15):4730–4738.
- [86] Li Y, Rios O, Kessler MR. Thermomagnetic processing of liquid-crystalline epoxy resins and their mechanical characterization using nanoindentation. *ACS Appl Mater Interfaces*. 2014;6(21):19456–19464.

- [87] Kotikian A, Truby RL, Boley JW, et al. *Adv Mater.* **2018**;30(10):6.
- [88] Davidson EC, Kotikian A, Li SC, et al. 3D printable and reconfigurable liquid crystal elastomers with light-induced shape memory via dynamic bond exchange. *Adv Mater.* **2020**;32(1):1905682.
- [89] Lopez-Valdeolivas M, Liu DQ, Broer DJ, et al. 4D printed actuators with soft-robotic functions. *Macromol. Rapid Commun.* **2018**;39(5):1700710.
- [90] Ambulo CP, Burroughs JJ, Boothby JM, et al. Four-dimensional printing of liquid crystal elastomers. *ACS Appl Mater Interfaces.* **2017**;9(42):37332–37339.
- [91] Mossety-Leszczak B, Strachota B, Strachota A, et al. The orientation-enhancing effect of diphenyl aluminium phosphate nanorods in a liquid-crystalline epoxy matrix ordered by magnetic field. *Eur Polym J.* **2015**;72:238–255.
- [92] Mossety-Leszczak B, Wlodarska M. Liquid-crystalline epoxy thermosets as matrices for ordered nanocomposites—a summary of experimental studies. *Polym Compos.* **2017**;38(2):277–286.
- [93] Mossety-Leszczak B, Kisiel M, Szalanski P, et al. The influence of a magnetic field on the morphology and thermomechanical properties of a liquid crystalline epoxy carbon composite. *Polym Compos.* **2018**;39: E2573–E2583.
- [94] Bae J, Jang J, Yoon SH. Cure behavior of the liquid-crystalline epoxy/carbon nanotube system and the effect of surface treatment of carbon fillers on cure reaction. *Macromol Chem Phys.* **2002**;203(15):2196–2204.
- [95] Chen S, Hsu SH, Wu MC, et al. Kinetics studies on the accelerated curing of liquid crystalline epoxy resin/multiwalled carbon nanotube nanocomposites. *J Polym Sci Part B – Polym Phys.* **2011**;49(4):301–309.
- [96] Luo X, Yu XY, Ma YH, et al. Preparation and cure kinetics of epoxy with nanodiamond modified with liquid crystalline epoxy. *Thermochim Acta.* **2018**;663:1–8.
- [97] Cai ZQ, Sun JZ, Ren H, et al. Effects of the heating rate and the amount of organic montmorillonite on the thermal Properties of the novel liquid crystalline epoxy nanocomposite. *Polym Plast Technol Eng.* **2008**;47(4):363–366.
- [98] Shanmugaraj AM, Ryu SH. Study on the effect of aminosilane functionalized nanoclay on the curing kinetics of epoxy nanocomposites. *Thermochim Acta.* **2012**;546:16–23.
- [99] Esmizadeh E, Naderi G, Yousefi AA, et al. Investigation of curing kinetics of epoxy resin/novel nanoclay–carbon nanotube hybrids by non-isothermal differential scanning calorimetry. *J Therm Anal Calorim.* **2016**;126(2):771–784.
- [100] Shen MM, Lu MG, Chen YL, et al. Effects of modifiers in organoclays on the curing reaction of liquid-crystalline epoxy resin. *J Appl Polym Sci.* **2005**;96(4):1329–1334.
- [101] Ha SM, Lee HL, Lee SG, et al. Thermal conductivity of graphite filled liquid crystal polymer composites and theoretical predictions. *Compos Sci Technol.* **2013**;88:113–119.
- [102] Zhang ZY, Zhang QK, Shen Z, et al. Synthesis and characterization of new liquid crystalline thermoplastic elastomers containing mesogen-jacketed liquid crystalline polymers. *Macromolecules.* **2016**;49(2):475–482.
- [103] Wang FF, Yao YM, Zeng XL, et al. Highly thermally conductive polymer nanocomposites based on boron nitride nanosheets decorated with silver nanoparticles. *RSC Adv.* **2016**;6(47):41630–41636.
- [104] Harada M, Hamaura N, Ochi M, et al. Thermal conductivity of liquid crystalline epoxy/BN filler composites having ordered network structure. *Compos Pt B-Eng.* **2013**;55:306–313.
- [105] Yang XT, Zhu JH, Yang D, et al. *Compos Pt B-Eng.* **2020**;185:107784.
- [106] Giang T, Kim J. Effect of backbone moiety in diglycidylether-terminated liquid crystalline epoxy on thermal conductivity of epoxy/alumina composite. *J Ind Eng Chem.* **2015**;30:77–84.
- [107] Yeo H, Islam AM, You NH, et al. Characteristic correlation between liquid crystalline epoxy and alumina filler on thermal conducting properties. *Compos Sci Technol.* **2017**;141:99–105.
- [108] Yeom YS, Cho KY, Seo HY, et al. *Compos Sci Technol.* **2020**;186:107915.
- [109] Carfagna C, Acierno D, Di Palma V, et al. Composites based on carbon fibers and liquid crystalline epoxy resins, 1 monomer synthesis and matrix curing. *Macromol Chem Phys.* **2000**;201(18):2631–2638.
- [110] Carfagna C, Meo G, Nicolais L, et al. Composites based on carbon fibers and liquid crystalline epoxy resins, 2 dynamic-mechanical analysis and fracture toughness behavior. *Macromol Chem Phys.* **2000**;201(18):2639–2645.
- [111] Sue HJ, Earls JD, Hefner RE, et al. Plummer: ‘morphology in diglycidyl ether of 4,4 ‘-dihydroxy-alpha-methylstilbene liquid crystalline epoxy composites. Lancaster: Technomic Publ Co Inc; 618–626; 1999.
- [112] Guo HL, Lu MG, Liang LY, et al. *J Appl Polym Sci.* **2014**;131(12):9.
- [113] Jang J, Bae J, Yoon SH. A study on the effect of surface treatment of carbon nanotubes for liquid crystalline epoxide–carbon nanotube composites. *J Mater Chem.* **2003**;13(4):676–681.
- [114] Hsu SH, Wu MC, Chen S, et al. Synthesis, morphology and physical properties of multi-walled carbon nanotube/biphenyl liquid crystalline epoxy composites. *Carbon N Y.* **2012**;50(3):896–905.
- [115] Lin YS, Hsu SLC, Ho TH, et al. *Polymers (Basel).* **2020**;12(9):1913.
- [116] Ambrogio V, Silvestre MG, Vito F, et al. Nanocomposites based on liquid crystalline resins. *Mol Cryst Liq Cryst.* **2005**;429:1–20.
- [117] Guo HL, Li YW, Zheng J, et al. High thermo-responsive shape memory epoxies based on substituted biphenyl mesogenic with good water resistance. *RSC Adv.* **2015**;5(82):67247–67257.
- [118] Rao YQ, Liu AD, O’Connell K. Barrier properties and structure of liquid crystalline epoxy and its nanocomposites. *Polymer (Guildf).* **2018**;142:109–118.
- [119] Jeong I, Kim CB, Kang DG, et al. Liquid crystalline epoxy resin with improved thermal conductivity by intermolecular dipole-dipole interactions. *J Polym Sci Part A – Polym Chem.* **2019**;57(6):708–715.
- [120] Shen WB, Wang L, Cao YP, et al. Cationic photopolymerization of liquid crystalline epoxide in mesogenic solvents and its application in polymer-stabilized liquid crystals. *Polymer (Guildf).* **2019**;172:231–238.

- [121] Nie L, Burgess A, Ryan A. Moisture permeation in liquid crystalline epoxy thermosets. *Macromol Chem Phys.* **2013**;214(2):225–235.
- [122] Kawamoto S, Fujiwara H, Nishimura S. Hydrogen characteristics and ordered structure of mono-mesogen type liquid-crystalline epoxy polymer. *Int J Hydrogen Energy.* **2016**;41(18):7500–7510.
- [123] Shen WB, Wang L, Chen G, et al. A facile route towards controllable electric-optical performance of polymer-dispersed liquid crystal via the implantation of liquid crystalline epoxy network in conventional resin. *Polymer (Guildf).* **2019**;167:67–77.
- [124] Shen WB, Cao YP, Zhang CH, et al. Network morphology and electro-optical characterisations of epoxy-based polymer stabilised liquid crystals. *Liq Cryst.* **2020**;47(4):481–488.
- [125] Hsu SH, Chen RS, Chang YL, et al. Biphenyl liquid crystalline epoxy resin as a low-shrinkage resin-based dental restorative nanocomposite. *Acta Biomater.* **2012**;8(11):4151–4161.
- [126] Giamberini M, Amendola E, Carfagna C. Curing of a rigid rod epoxy resin with an aliphatic diacid: an example of a lightly crosslinked liquid crystalline thermoset. *Macromol Rapid Commun.* **1995**;16(2):97–105.
- [127] Belmonte A, Lama GC, Gentile G, et al. Thermally-triggered free-standing shape-memory actuators. *Eur Polym J.* **2017**;97:241–252.
- [128] Belmonte A, Lama GC, Gentile G, et al. Synthesis and characterization of liquid-crystalline networks: toward autonomous shape-memory actuation. *J Phys Chem C.* **2017**;121(40):22403–22414.
- [129] Belmonte A, Lama GC, Cerruti P, et al. Motion control in free-standing shape-memory actuators. *Smart Mater Struct.* **2018**;27(7):17.
- [130] Li Y, Zhang Y, Rios O, et al. Liquid crystalline epoxy networks with exchangeable disulfide bonds. *Soft Matter.* **2017**;13(29):5021–5027.
- [131] Li Y, Zhang Y, Rios O, et al. Photo-responsive liquid crystalline epoxy networks with exchangeable disulfide bonds. *RSC Adv.* **2017**;7(59):37248–37254.
- [132] Chen QM, Li YS, Yang Y, et al. Durable liquid-crystalline vitrimer actuators. *Chem Sci.* **2019**;10(10):3025–3030.
- [133] Liu XF, Luo X, Liu BW, et al. Toughening epoxy resin using a liquid crystalline elastomer for versatile application. *ACS Appl Polym Mater.* **2019**;1(9):2291–2301.
- [134] Yang Y, Terentjev EM, Zhang YB, et al. Reprocessable thermoset soft actuators. *Angew Chem Int Ed.* **2019**;58(48):17474–17479.
- [135] Pei Z, Yang Y, Chen Q, et al. Regional shape control of strategically assembled multishape memory vitrimers. *Adv Mater.* **2016**;28(1):156–160.
- [136] Yang Y, Pei ZQ, Li Z, et al. Making and remaking dynamic 3D structures by shining light on flat liquid crystalline vitrimer films without a mold. *J Am Chem Soc.* **2016**;138(7):2118–2121.
- [137] Wang HM, Yang Y, Zhang MC, et al. Electricity-triggered self-healing of conductive and thermostable vitrimer enabled by paving aligned carbon nanotubes. *ACS Appl Mater Interfaces.* **2020**;12(12):14315–14322.
- [138] Lama GC, Cerruti P, Lavorgna M, et al. Controlled actuation of a carbon nanotube/epoxy shape-memory liquid crystalline elastomer. *J Phys Chem C.* **2016**;120(42):24417–24426.
- [139] Marotta A, Lama GC, Ambrogio V, et al. Shape memory behavior of liquid-crystalline elastomer/graphene oxide nanocomposites. *Compos Sci Technol.* **2018**;159:251–258.
- [140] Li Y, Rios O, Keum JK, et al. Photoresponsive liquid crystalline epoxy networks with shape memory behavior and dynamic ester bonds. *ACS Appl Mater Interfaces.* **2016**;8(24):15750–15757.
- [141] Lu XL, Guo SW, Tong X, et al. *Adv Mater.* **2017**;29(28):7.
- [142] Lu XL, Zhang H, Fei GX, et al. *Adv Mater.* **2018**;30(14):8.